

Review

Recent Advances in Understanding *R*-Process Nucleosynthesis in Metal-Poor Stars and Stellar Systems

Avrajit Bandyopadhyay ^{1,*}  and Timothy C. Beers ^{2,†} 
¹ Department of Astronomy, University of Florida, Gainesville, FL 32611, USA

² Department of Physics and Astronomy, University of Notre Dame, Notre Dame, IN 46556, USA; tbeers@nd.edu

* Correspondence: avrajit.ban@gmail.com or abandyopadhyay@ufl.edu

† These authors contributed equally to this work.

Abstract

The rapid neutron-capture process (*r*-process) is responsible for the creation of roughly half of the elements heavier than iron, including precious metals like silver, gold, and platinum, as well as radioactive elements such as thorium and uranium. Despite its importance, the nature of the astrophysical sites where the *r*-process occurs, and the detailed mechanisms of its formation, remain elusive. The key to resolving these mysteries lies in the study of chemical signatures preserved in ancient, metal-poor stars. These stars, which formed in the early Universe, retain the chemical fingerprints of early nucleosynthetic events and offer a unique opportunity to trace the origins of *r*-process elements in the early Galaxy. In this review, we explore the state-of-the-art understanding of *r*-process nucleosynthesis, focusing on the sites, progenitors, and formation mechanisms. We discuss the role of potential astrophysical sites such as neutron star mergers, core-collapse supernovae, magneto-rotational supernovae, and collapsars, that can play a key role in producing the heavy elements. We also highlight the importance of studying these signatures through high-resolution spectroscopic surveys, stellar archaeology, and multi-messenger astronomy. Recent advancements, such as the gravitational wave event GW170817 and detection of the *r*-process in the ejecta of its associated kilonovae, have established neutron star mergers as one of the confirmed sites. However, questions remain regarding whether they are the only sites that could have contributed in early epochs or if additional sources are needed to explain the signatures of *r*-process found in the oldest stars. Additionally, there are strong indications pointing towards additional sources of *r*-process-rich nuclei in the context of Galactic evolutionary timescales. These are several of the outstanding questions that led to the formation of collaborative efforts such as the *R*-Process Alliance, which aims to consolidate observational data, modeling techniques, and theoretical frameworks to derive better constraints on deciphering the astrophysical sites and timescales of *r*-process enrichment in the Galaxy. This review summarizes what has been learned so far, the challenges that remain, and the exciting prospects for future discoveries. The increasing synergy between observational facilities, computational models, and large-scale surveys is poised to transform our understanding of *r*-process nucleosynthesis in the coming years.

Keywords: nucleosynthesis; *r*-process; neutron capture processes; metal-poor stars; chemical abundances; globular clusters; dwarf galaxies; core-collapse supernovae; neutron star mergers



Academic Editor: Giuseppe Verde

Received: 5 May 2025

Revised: 9 June 2025

Accepted: 7 July 2025

Published: 11 July 2025

Citation: Bandyopadhyay, A.; Beers, T.C. Recent Advances in Understanding *R*-Process Nucleosynthesis in Metal-Poor Stars and Stellar Systems. *Universe* **2025**, *11*, 229. <https://doi.org/10.3390/universe11070229>

Copyright: © 2025 by the authors. Licensee MDPI, Basel, Switzerland. This article is an open access article distributed under the terms and conditions of the Creative Commons Attribution (CC BY) license (<https://creativecommons.org/licenses/by/4.0/>).

1. Introduction

Ancient, metal-poor stars serve as “cosmic fossils”, as they are formed primarily within the first few billion years following the Big Bang. They are low mass, long-lived, and retain detailed records of their past host environments, allowing us to reconstruct the chemical evolution of the Galaxy [1–6]. These metal-poor stars (stars with lower content of metals compared to the Sun; in astronomy all elements heavier than H and He are referred to as “metals”) provide crucial insight into the nucleosynthetic processes and star-formation histories of the first generations of stars in the early Milky Way, as they retain the chemical signatures from their progenitors. With high-resolution spectroscopic studies of these metal-poor stars, it is possible to throw light on the possible enrichment events in the early Galaxy and its chemical evolution.

The elemental signatures imprinted in these stars encode information about their progenitors and past nucleosynthetic events, including possible contributions from neutron star–neutron star and neutron star–black hole mergers, core-collapse supernovae, and other enrichment sources. Over the past decade, the advent of large-scale observational surveys (e.g., SDSS, LAMOST, GALAH, and DESI), along with advances in theoretical models and experimental data, have ushered in a renaissance in the field of Galactic Archaeology, providing unprecedented insight into the chemical–evolutionary history of the Milky Way and its satellite galaxies [7–9]. This progress has established a crucial link between nuclear astrophysics, stellar evolution, and galaxy formation, enabling us to place stringent constraints on the physical processes driving chemical enrichment in the cosmos. In particular, the most metal-poor stars in the Milky Way halo—remnants of the early Universe—offer a unique opportunity to probe the nucleosynthetic pathways that governed the formation of the heaviest elements [6,10]. These stars, largely chemically undisturbed over some 12–13 Gyr, act as pristine records of the earliest enrichment events, preserving the chemical fingerprints of individual nucleosynthetic processes that are otherwise difficult to disentangle from studies of younger or more metal-rich stars [11,12].

By studying the elemental compositions of these ancient stars, we endeavor to isolate the distinct contributions from the proposed astrophysical enrichment events. Unlike laboratory nuclear physics experiments, which cannot replicate the extreme environments required for the production of the heaviest elements, these stars serve as natural testbeds for understanding *r*-process nucleosynthesis and the chemical evolution of the Universe. Their elemental-abundance patterns provide crucial insights into how heavy elements shaped the formation and evolution of stars and galaxies and link the present-day Milky Way to its complex accretion history.

Hydrogen, helium, and a tiny amount of lithium are formed through nucleosynthesis in the Big Bang, but their relative abundances are influenced by later processing in stellar interiors [13–15]. Beryllium and boron arise from spallation reactions in the interstellar medium. All other elements up to the iron peak are synthesized through nuclear fusion within stellar interiors or explosive nucleosynthesis in supernovae, as shown in Figure 1.

In contrast, heavier elements ($Z > 30$) are primarily formed through neutron-capture processes [8,16]. The rapid neutron-capture process (*r*-process) occurs in extreme conditions with high neutron flux, where the neutron-capture rate surpasses the beta-decay rate, leading to the formation of neutron-rich nuclei that subsequently decay to stability, producing the heaviest natural elements up to uranium. Approximately half of all stable isotopes of elements beyond the iron peak originate from this process, while the remaining half is produced through the slow neutron-capture process (*s*-process) or the intermediate neutron-capture process (*i*-process), both of which operate at different but lower neutron densities and are thought to be primarily associated with asymptotic giant branch (AGB) stars. While the astrophysical sites of the *s*-process are relatively well understood

and progress is being made on understanding that of the *i*-process, the dominant site of the *r*-process remains a topic of active debate, with neutron star mergers being the only confirmed source. Other astrophysical sites of the *r*-process may also contribute, in as-yet not understood fractions.

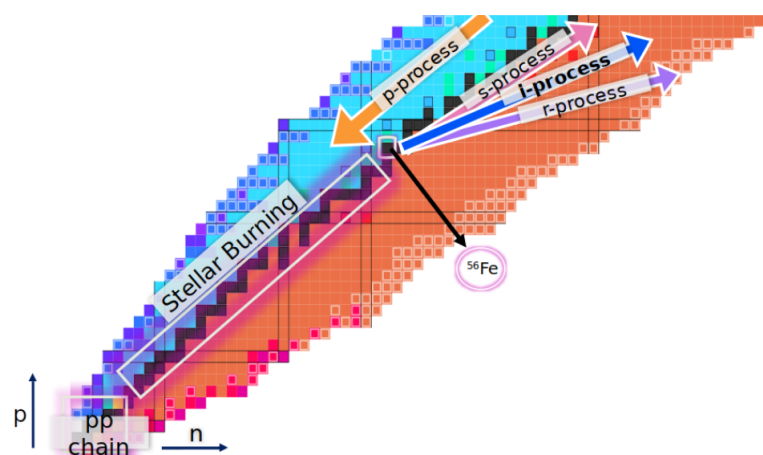


Figure 1. A portion of the chart of nuclides, illustrating the different nucleosynthetic pathways in stars. Key nuclear burning processes such as the p-p chain or proton-capture reactions, and advanced burning stages, are shown alongside regions where nucleosynthesis proceeds via neutron capture. The iron (Fe) peak is marked to indicate the transition beyond which elements are predominantly produced through slow (*s*-process), intermediate (*i*-process), or rapid (*r*-process) neutron capture. Credit: S. Uthayakumar, Facility for Rare Isotope Beams, Michigan State University, East Lansing, Michigan 48824, USA. Nuclide chart (<https://people.physics.anu.edu.au/~ecs103/chart/>, accessed on 6 July 2025) by E. C. Simpson, Australian National University. This figure is reproduced with due permission.

Thus, the formation of elements in the Universe is governed by a complex interplay of nucleosynthesis processes that span a wide range of astrophysical environments. A fundamental challenge in astrophysics is to decipher the relative contributions of these processes to the chemical enrichment of the Milky Way and to identify the astrophysical sites responsible for heavy-element production. Recent advancements in high-resolution spectroscopy have revolutionized our ability to probe the first generations of stars by enabling detailed elemental-abundance measurements, in particular for the *r*-process-enhanced (RPE) stars identified by the *R*-Process Alliance (RPA) [17–24]. These abundances serve as powerful tracers of the mass and explosion energies of the progenitor population(s), providing critical insights into the early initial mass function (IMF) and the chemical evolution of the Galaxy. However, a comprehensive understanding linking the nucleosynthesis of both light and heavy elements with the accretion history of the Galaxy, particularly across different stellar environments, in order to trace the original sites of the *r*-process or early enrichment events and their relative contributions as a function of time, remains incomplete.

As noted above, the formation of *r*-process elements requires extreme conditions with high neutron fluxes, limiting their production sites to core-collapse supernovae, magneto-rotationally jet-driven supernovae, and neutron star mergers (NSMs) or neutron star–black hole mergers [25].¹

The recent detection of *r*-process elements in kilonovae following gravitational wave events [27] has conclusively identified NSMs as at least one site of *r*-process nucleosynthesis [28]. However, the presence of RPE stars at very low metallicities suggests that heavy-element enrichment occurred early in the Universe. Such enrichments are likely to be preserved in environments with minimal subsequent star formation, such as in low-mass dwarf galaxies. Variations in *r*-process dilution levels within natal gas clouds likely

influenced the observed dispersion in r -process enhancements, as stars with higher $[\text{Fe}/\text{H}]$ may have formed in higher-mass systems where the r -process yields were more diluted or where multiple progenitors contributed to enrichment.

The robust universality of the main r -process pattern (near the second neutron-capture peak, containing elements like Eu, Ba, and others; see Figure 2) across stars of all metallicities points to a dominant production mechanism (see [7]). However, the large scatter in light r -process elements (first neutron-capture peak) and the presence of the so-called actinide-boost stars (stars that exhibit unusually high abundances of thorium and uranium relative to stable 2nd-peak elements such as europium) suggest multiple enrichment sites [29–31]. Observations of RPE ultra-faint dwarf (UFD) galaxies such as Reticulum II (Ret II; [32–34]) further indicate that at least some of these sites contributed to rapid and early chemical enrichment, raising fundamental questions about the relative roles and timescales of different nucleosynthetic pathways in shaping the Milky Way’s chemical evolution.

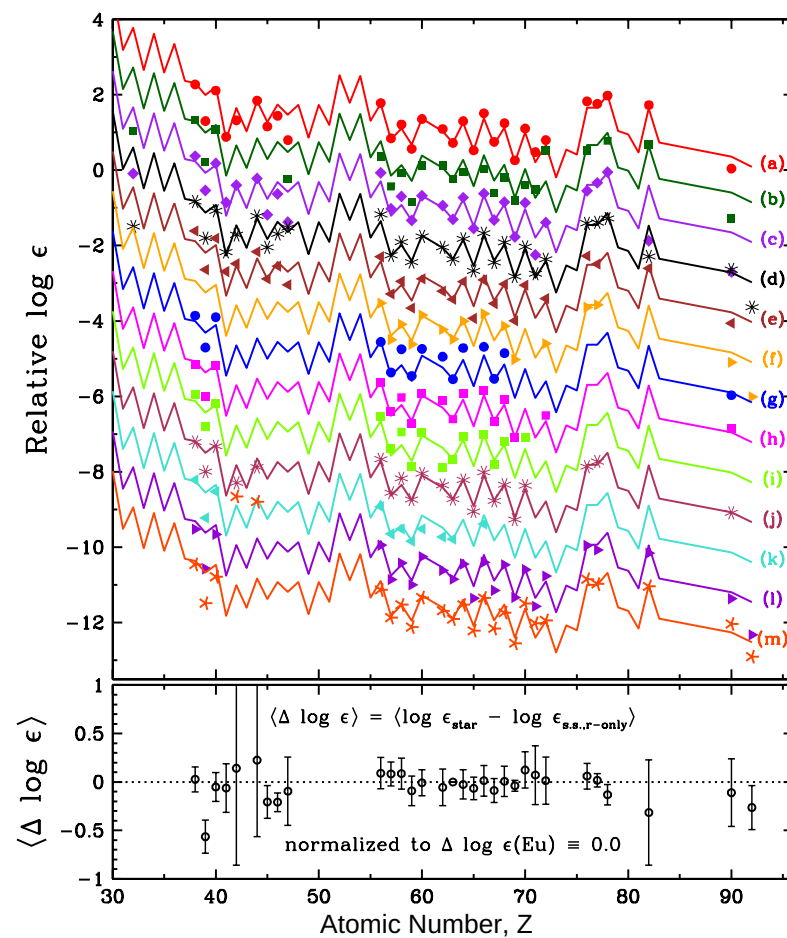


Figure 2. This figure, from [7], shows the robustness of the main r -process. Note that $\log \epsilon(X) = \log_{10} (N_X/N_H) + 12$, where N_X and N_H represent the number densities of element X and hydrogen, respectively. Top panel: neutron-capture element abundances in 13 r -process-enhanced stars (individual data points), compared with the scaled Solar System r -process-only abundance pattern from [19], primarily based on values from [35]. All distributions have been normalized to match the europium abundance ($Z = 63$), with additional vertical offsets applied to individual stellar patterns for clarity. Bottom panel: mean differences between the stellar abundances and the Solar System r -process pattern across the 13 stars. This figure is reproduced with permission and was originally published in *Reviews of Modern Physics*.

To fully understand the cosmic origins of the astrophysical r -process, it is crucial to identify stars from partially or totally disrupted dwarf galaxies by taking advantage of

precisely measured stellar dynamics and employing them to trace their chemical evolution. The enrichment levels of their *r*-process signatures coming from diverse sources (assuming more than one process contributes) will place valuable constraints on the role of NSMs in early epochs. Questions we need to address include whether NSMs were prolific across many progenitor satellite galaxies or do we need additional astrophysical sites to explain the observed *r*-process signatures? Furthermore, investigating the contributions from supernovae in these disrupted systems using the Fe-peak (elements in the periodic table around Fe such as Mn, Cr, Co, and Ni) and α -elements (such as O, Mg, and Ca, which are produced by α -capture reactions) will help determine the timescales of *r*-process enrichment and whether multiple nucleosynthetic pathways were necessary to shape their chemical evolution.

2. Signatures of the *r*-Process in Stars

The *r*-process is (likely primarily) responsible for the formation of the heaviest elements in the Universe. This process unfolds in environments with extreme neutron densities, typically exceeding $n_n > 10^{22} \text{ cm}^{-3}$, where seed nuclei rapidly absorb neutrons. As a result, highly neutron-rich isotopes form far from the valley of stability. Within just a few seconds, these isotopes undergo a cascade of neutron captures before the neutron flux ceases, triggering radioactive decay that stabilizes them into heavy elements such as thorium ($Z = 90$) and uranium ($Z = 92$). Despite advances in nuclear physics and astrophysical modeling, predicting precise *r*-process abundance patterns remains a challenge. However, observational data, particularly from the Sun and ancient, metal-poor stars, reveals a distinct distribution of *r*-process elements [36].

A defining feature of the *r*-process is its characteristic abundance signatures, which consists of three major peaks in the relative abundances of elements (see Figure 3). The first peak, around $Z = 34\text{--}40$ (strontium, yttrium, and zirconium, among others), the second near $Z = 56\text{--}70$ (barium, cesium, europium, and others), and the third around $Z = 76\text{--}78$ (e.g., osmium, iridium, and platinum) arise due to the delayed β decay² of neutron-rich progenitors with closed neutron shells. This mechanism fundamentally differs from the *s*-process, where neutron-magic nuclei accumulate at stable configurations, creating different peak structures.

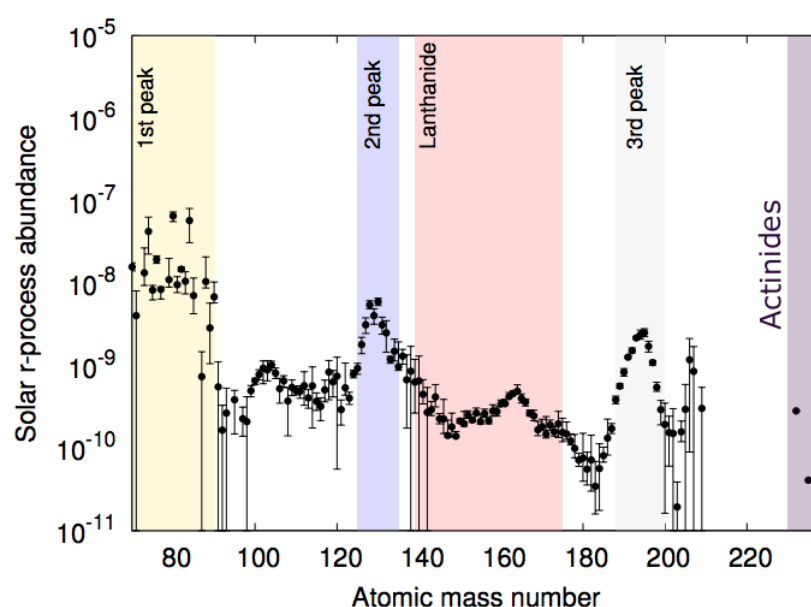


Figure 3. The three distinct *r*-process peaks as a function of the atomic mass number as observed in the Sun. The black filled circles represent the observed abundances corresponding to the atomic mass

number along with the uncertainties. This Figure was edited by E. M. Holmbeck, adapted from [37] with due permission from K. Hotokezaka, and was originally published in the *International Journal of Modern Physics D*.

For reference, Table 1 summarizes the current definitions of the enrichment levels of stars, based on their iron-to-hydrogen ratios, relative to that of the Sun.³ Note that, at present, the lowest metallicity stars have an evaluated upper limit (not detections) that approach $[\text{Fe}/\text{H}] = -8.0$, one hundred million times lower than the Solar level [38]. Such upper limits are crucial to understand the enrichment processes and timescales of the early stellar populations and possibly the first stars. The lowest metallicity RPE stars found to date occur at $[\text{Fe}/\text{H}] \sim -3$ to ~ -4.0 . None have yet been identified significantly below $[\text{Fe}/\text{H}] = -4.0$. This table also summarizes the different signatures of neutron-capture processes known at present and the contemporary definition of carbon-enhanced metal-poor (CEMP) stars.

Table 1. Classes and signatures of metal-poor stars.

Description	Definition	Abbreviation
Solar	$[\text{Fe}/\text{H}] = 0.0$	
Metal-poor	$[\text{Fe}/\text{H}] \leq -1.0$	MP
Very metal-poor	$[\text{Fe}/\text{H}] \leq -2.0$	VMP
Extremely metal-poor	$[\text{Fe}/\text{H}] \leq -3.0$	EMP
Ultra metal-poor	$[\text{Fe}/\text{H}] \leq -4.0$	UMP
Hyper metal-poor	$[\text{Fe}/\text{H}] \leq -5.0$	HMP
Mega metal-poor	$[\text{Fe}/\text{H}] \leq -6.0$	MMP
Septa metal-poor	$[\text{Fe}/\text{H}] \leq -7.0$	SMP
Octa metal-poor	$[\text{Fe}/\text{H}] \leq -8.0$	OMP
Giga metal-poor	$[\text{Fe}/\text{H}] \leq -9.0$	GMP
Signature	Criteria	Abbreviation
<i>r</i> -process-enhanced	$+0.3 < [\text{Eu}/\text{Fe}] \leq +0.70$ and $[\text{Ba}/\text{Eu}] < 0.0$	<i>r</i> -I
	$[\text{Eu}/\text{Fe}] > +0.7$ and $[\text{Ba}/\text{Eu}] < 0.0$	<i>r</i> -II
limited <i>r</i> -process	$[\text{Eu}/\text{Fe}] \leq +0.3$, $[\text{Sr}/\text{Ba}] > +0.5$, and $[\text{Sr}/\text{Eu}] > 0.0$	r_{lim}
<i>s</i> -process:	$[\text{Ba}/\text{Fe}] > +1.0$, $[\text{Ba}/\text{Eu}] > +0.5$; also $[\text{Ba}/\text{Pb}] > -1.5$	<i>s</i>
<i>r</i> - and <i>s</i> -process	$0.0 < [\text{Ba}/\text{Eu}] < +0.5$ and $-1.0 < [\text{Ba}/\text{Pb}] < -0.5$	<i>r/s</i>
<i>i</i> -process	$0.0 < [\text{La}/\text{Eu}] < +0.6$ and $[\text{Hf}/\text{Ir}] \sim +1.0$	<i>i</i>
carbon-enhanced	$[\text{C}/\text{Fe}] > +0.7$	CEMP

The presence of *r*-process elements in extremely metal-poor ($[\text{Fe}/\text{H}] \leq -3.0$) stars confirms that this process was active in the early Universe. These rare stars serve as fossil records of ancient nucleosynthesis, preserving the chemical imprints of past *r*-process events. Large-scale surveys suggest that only 3–5% of stars with $[\text{Fe}/\text{H}] < -2.5$ in the Galactic halo system exhibit strong *r*-process enhancement [10,18,20–24]. These stars did not synthesize neutron-capture elements themselves; rather, they inherited them from an earlier generation of stellar explosions. The striking similarity between the main *r*-process patterns in these stars and the Solar *r*-process signature suggests a common nucleosynthetic origin.

The degree of *r*-process enrichment in metal-poor stars is commonly measured using the europium-to-iron ratio relative to the Sun, $[\text{Eu}/\text{Fe}]$, which serves as a proxy for neutron-capture element production [4]. Based on this metric, RPE stars are classified into two primary categories: *r*-I stars, with moderate enhancement ($+0.3 < [\text{Eu}/\text{Fe}] \leq +0.7$) and *r*-II stars, which exhibit strong enhancement ($[\text{Eu}/\text{Fe}] > +0.7$). The latter group, with eu-

roplum levels more than five times the Solar value, provides compelling evidence for localized *r*-process events. Some of the most well-known *r*-II stars include CS 22892-052 [39], the first identified *r*-II star with $[\text{Fe}/\text{H}] \lesssim -3.0$. This star is also enhanced in carbon (and hence can be classified as CEMP-*r*, following the nomenclature of [4]). Others include CS 31082-001 [40], which is not carbon enhanced but exhibits thorium, uranium, and an actinide boost (described below), and HE 1523-0901 [41], which also contains uranium. These stars, despite their extremely low metallicities, exhibit an enrichment of neutron-capture elements by factors of 40–70 relative to iron. Note also that there are a few metal-poor stars with enrichment levels exceeding 100 (e.g., 2MASS J15213995-3538094 [42] and 2MASS J22132050-5137385 [43]), which are sometimes referred to as *r*-III ($[\text{Eu}/\text{Fe}] > +2.0$) stars [44]; this definition may shift as more such stars are identified.

The chemical-enrichment history of these stars rules out localized atmospheric effects as the cause of their *r*-process signatures. Radial velocity monitoring studies (e.g., [45] and references therein) reveal that approximately 80% of RPE stars exhibit no evidence of binary motion, eliminating mass transfer from a companion as a likely explanation. Instead, their neutron-capture enrichment reflects the properties of the natal gas clouds from which they formed, shaped by prior supernovae or NSMs. However, the existence of actinide-boost stars (e.g., [33,46–49]) complicates this picture, hinting at possible variations in *r*-process yields or multiple contributing astrophysical sources. See Figure 4.

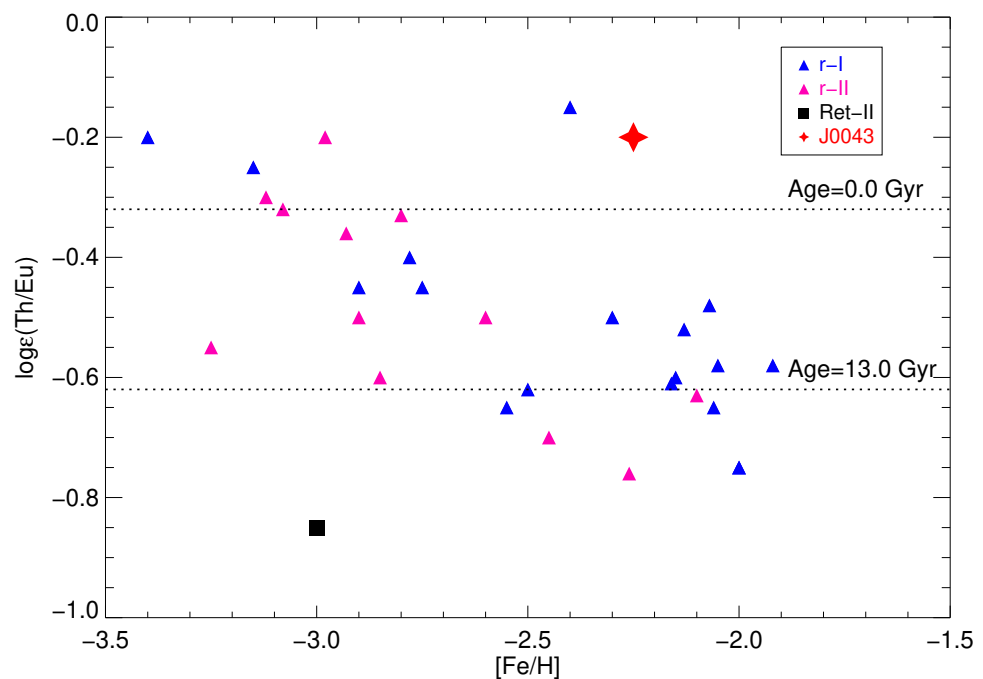


Figure 4. Distribution of $\log \epsilon(\text{Th}/\text{Eu})$ for metal-poor stars as a function of $[\text{Fe}/\text{H}]$. Previously recognized *r*-I (blue triangles) and *r*-II (pink triangles) stars are shown for comparison, along with a bright *r*-II star (black square) from a dwarf galaxy. Dashed lines indicate corresponding ages derived from the $[\text{Th}/\text{Eu}]$ ratios. Stars with unusually high Th relative to Eu, known as actinide-boost stars, occupy the upper region of the diagram and yield un-physically young ages due to their elevated $[\text{Th}/\text{Eu}]$ values. Figure adapted from [30], reproduced with permission © AAS.

Recent observational evidence suggests that fission fragments from transuranic nuclei may significantly influence the observed abundance patterns of RPE stars. Ref. [50] analyzed a sample of 42 RPE stars and identified strong correlations between the abundances of certain lighter ($Z = 44\text{--}47$) and heavier ($Z = 63\text{--}78$) *r*-process elements. These correlations, not seen for adjacent atomic numbers, are inconsistent with traditional two-component

r-process models, and are instead interpreted as signatures of fission products originating from very neutron-rich nuclei with mass numbers exceeding 260. The presence of nearly constant abundance ratios, such as [Ag/Eu], across the stellar sample further supports the role of fission in smoothing out variations introduced by initial conditions at the nucleosynthesis site. This highlights fission as a potentially universal feature in *r*-process events, such as neutron star mergers, contributing to the chemical makeup of the early Galaxy.

The broader population of RPE stars spans a metallicity range of $-4.0 < [\text{Fe}/\text{H}] < -1.5$. However, at a metallicity of ~ -1.5 , the median [Eu/Fe] among Galactic halo stars drops to approximately +0.3 [16]. At this point, nearly 50% of stars satisfy the *r*-I classification, making the definition of RPE stars less distinct. To confirm whether these stars genuinely reflect an *r*-process enrichment history, one must examine their complete neutron-capture element abundance patterns. The influence of other nucleosynthetic pathways, such as from the *s*-process, becomes evident at higher metallicities.

Despite considerable progress, the identification of *r*-process production sites remains an open question. New observational and theoretical developments continue to refine our understanding of how and where these elements are synthesized. The next sections explore the most promising astrophysical candidates, focusing on core-collapse supernovae, magneto-rotational explosions, and neutron star mergers, and their respective contributions to Galactic chemical evolution.

3. Astrophysical Sites for the Production of *r*-Process Elements

The fundamental question in *r*-process nucleosynthesis is identifying the astrophysical sites responsible for producing heavy elements via rapid neutron capture [9,51–53]. The primary requirement for an *r*-process site is an environment with an abundant neutron supply, ensuring a sufficiently high neutron-to-seed ratio for the synthesis of heavy nuclei [16]. Several astrophysical events have been proposed as potential *r*-process sites, each contributing to different phases of cosmic evolution.

One of the key physical parameters used to distinguish *r*-process sites is the neutron-to-seed ratio, usually quantified by the electron fraction (Y_e). Higher neutron-to-seed ratios lead to lower Y_e and vice versa. A low electron fraction ($Y_e < 0.10$), corresponding to high neutron densities, results in the formation of the heaviest nuclei, including the third *r*-process peak (e.g., actinides such as thorium and uranium). In contrast, environments with moderate electron fractions predominantly produce elements associated with the main *r*-process, while higher electron fractions ($Y_e > 0.25$) lead to the synthesis of only the first *r*-process peak elements. However, additional processes and mechanisms, such as the *s*-process and the *i*-process, can also contribute to elements near the first peak (and beyond for the *i*-process; see Figure 5), necessitating a careful assessment of their origins.

Among the most widely considered astrophysical sites for *r*-process nucleosynthesis are core-collapse supernovae and binary neutron star mergers, along with other potential sources such as collapsars (massive star collapses leading to black holes with accretion disks) and neutron star–black hole mergers, which may also contribute to *r*-process elements under specific conditions.

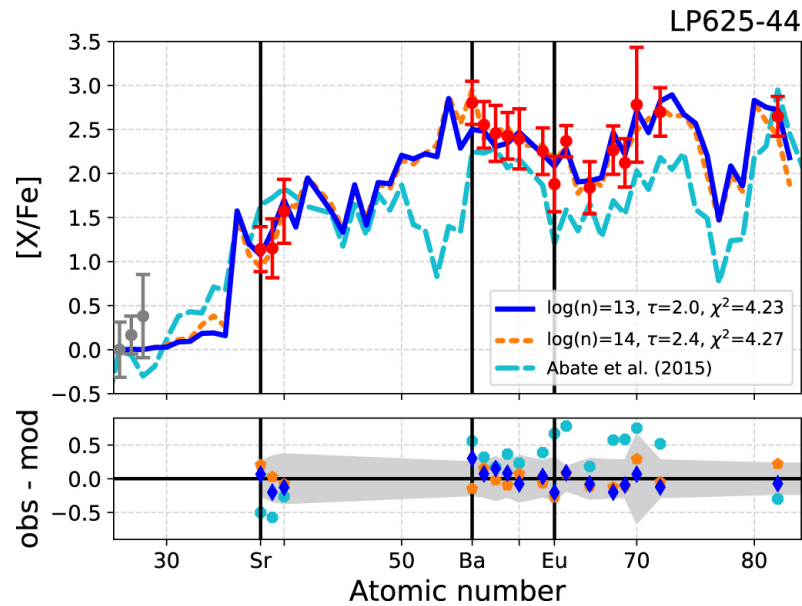


Figure 5. Best fits to the heavy-element abundance pattern of the CEMP-*i* star LP625-44. In this figure, taken from [54], the blue and orange lines represent the best-fitting *i*-process models with neutron densities of $n = 10^{15} \text{ cm}^{-3}$ and $n = 10^{14} \text{ cm}^{-3}$, respectively. The lower panel shows the residuals of the measured abundances from the adopted *i*-process model, with the expected range of uncertainties in the model indicated in shaded gray. This figure is reproduced with permission © AAS and was originally published in *The Astrophysical Journal*.

3.1. Neutron Star Mergers

NSMs are widely recognized as a key site for *r*-process nucleosynthesis, where rapid neutron captures form the heaviest elements in the Universe. These mergers occur when two compact objects, such as neutron stars or a neutron star and a black hole, gradually spiral inwards while losing energy through gravitational wave emission. The ground-breaking gravitational wave detection GW170817 [27], accompanied by the kilonova AT2017gfo [55,56], provided definitive observational evidence that binary neutron star (BNS) mergers can produce heavy *r*-process elements. The detection of strontium in the electromagnetic counterpart confirmed the synthesis of lighter *r*-process nuclei [28], while the broad-band light curves [55] and spectral evolution [57] indicated the presence of both light and heavy *r*-process components. A summary of the multi-messenger results from this event is provided by [27].

BNS mergers are expected to eject roughly $0.01 M_{\odot}$ of neutron-rich material during the collision, with the precise ratio of light-to-heavy *r*-process elements varying based on the ejecta's neutron fraction and the mass and spin of the compact objects (e.g., [58] and references therein). Simulations have shown that BNS mergers can generate significant amounts of both the first and second *r*-process peak elements, while neutron star–black hole (NSBH) mergers could play a more substantial role in forming the heaviest *r*-process species [59,60], depending on the black hole's spin and the tidal disruption dynamics [61]. However, the overall contribution of NSMs to the Galactic *r*-process inventory remains debated, as their suggested delayed timescales and potential for substantial velocity kicks may cause enrichment to occur long after or far away from the formation of many stars.

The delay time between the formation of the progenitor stars and the actual merger event is governed by the timescale required for the system to lose energy through gravitational radiation. Population-synthesis models suggest that most NSMs occur with a delay of tens to hundreds of millions of years, although a small fraction may merge rapidly, within a few Myr [62,63]. These variations complicate the role of NSMs in early Galactic chemical evolution, as mergers with longer delay times may not contribute to the *r*-process

enrichment of low-metallicity stars. Recent studies indicate that NSBH mergers, with their shorter in-spiral timescales and higher ejecta masses, may have played a more significant role in enriching the early Milky Way with r -process elements [60,64].

As noted above, despite the clear evidence that NSMs produce r -process material, their overall contribution to the Galactic r -process inventory is still uncertain. Some chemical-evolution models, such as those by [8,37], suggest that NSMs alone cannot account for the entire r -process abundance distribution, particularly at low metallicities. These models indicate that mergers would need to occur with unusually short delay times or exceptionally high ejecta masses to explain the observed europium distribution in metal-poor stars. Alternatively, an additional astrophysical site, such as rare magneto-rotational supernovae or neutron star–white dwarf (NSWD) mergers, may be required to fully account for the Galactic r -process enrichment.

Recent observations of kilonova-like transients following long-duration gamma-ray bursts (GRBs), such as GRB 211211A and GRB 230307A, have sparked interest in NSWD mergers as potential r -process sites [65]. However, current estimates suggest that NSWD mergers eject significantly less neutron-rich material than NSMs or NSBH mergers, likely contributing less than $0.0005 M_{\odot}$ of r -process material per event, making them an unlikely dominant source [66].

Three-dimensional magneto-hydrodynamic simulations of NSM remnants have revealed that the neutron-rich ejecta exhibit a broad range of Y_e , spanning from ~ 0.25 to 0.40 . This diversity leads to an r -process abundance pattern that does not perfectly match the Solar pattern, as the production of the heaviest r -process species remains limited. Ref. [58] further demonstrated that the present-day Galactic population of BNS systems tends to favor the production of lighter r -process elements, which could imply the need for additional sites to explain the Solar System's abundance of the heaviest r -process species.

Overall, while NSMs are confirmed as prolific r -process factories, ongoing debate persists regarding their relative importance. Their suggested delayed timescales, potential for high-velocity kicks, and the challenges in reconciling their yields with observed stellar abundances indicate that complementary astrophysical sites may still be required to fully explain the origin of the heaviest elements in the Milky Way.

3.2. Core-Collapse Supernovae

The idea that core-collapse supernovae (CC-SNe) are potential sites for r -process nucleosynthesis has been explored since the pioneering work of [67,68]. However, subsequent observations and models (e.g., [69]) have shown that not all supernovae are equally capable of producing r -process elements. Instead, only a small fraction, estimated at around 1–10%, of core-collapse events may generate the conditions necessary for synthesizing heavy r -process nuclei [70–72], including those around the second and third abundance peaks. This implies that r -process nucleosynthesis in CC-SNe is relatively rare but potentially plays a significant role in Galactic chemical evolution.

Several mechanisms have been proposed to explain how CC-SNe might produce the full range of r -process elements. One of the most studied scenarios involves neutrino-driven winds emanating from the proto neutron star [73]. As the star collapses, intense neutrino fluxes expel neutron-rich material, creating conditions suitable for rapid neutron capture. Electron-capture supernovae, originating from progenitors with masses between roughly 8 and $10 M_{\odot}$, have also been considered as potential r -process sites [74]. However, modern hydrodynamical simulations indicate that these mechanisms often fail to generate the neutron richness required for a complete r -process, instead producing a weaker r -process that is limited to lighter neutron-capture elements near the first r -process peak [75–77]. This

limited r -process is believed to occur more frequently, and may well account for the light neutron-capture elements such as Sr, Y, and Zr observed in some metal-poor stars.

From an observational perspective, metal-poor stars that exhibit signatures of a limited r -process provide key insights [78–80] on the possible progenitors such as CC-SNe [81]. These stars, now classified as “limited r -process stars,” exhibit abundance patterns characterized by $[\text{Eu}/\text{Fe}] \leq +0.3$, $[\text{Sr}/\text{Ba}] > +0.5$, and $[\text{Sr}/\text{Eu}] > 0.0$ [23]. The chemical signatures of these stars suggest that they formed from gas enriched by weak r -process events, likely from CC-SNe. Theoretical models propose that this limited r -process originates from a quasi-statistical equilibrium (QSE) phase with a relatively low neutron-to-seed ratio (<100), which prevents the synthesis of heavier r -process elements. Consequently, only lighter neutron-capture elements near the first peak are produced, with rapidly diminishing yields toward the second peak [80].

The weak r -process also operates on even shorter timescales compared to the main r -process. In such environments, often associated with neutrino-driven winds or early core-collapse supernovae, (α, n) reactions can play a critical role by enabling the material to reach higher atomic numbers, effectively bridging gaps that would otherwise require slow β -decays. This pathway has attracted considerable attention, both theoretically and experimentally, with recent work focusing on reaction rates and nuclear inputs relevant to light trans-iron nuclei. These developments help refine predictions for the light r -process element patterns observed in many metal-poor stars. For more details, see [82–84].

Recent studies using magneto-hydrodynamical simulations have added new insights into r -process production in CC-SNe. Models by [70] explore the role of rotation and magnetic fields in influencing the nucleosynthesis outcomes. Their work identifies two explosion scenarios: prompt magnetic-jet and delayed magnetic-jet explosions. In the prompt magnetic-jet case, where the magnetic fields are particularly strong, heavy r -process elements, including actinides, are synthesized. In contrast, the delayed magnetic-jet explosions, associated with weaker magnetic fields, tend to produce only lighter r -process nuclei, up to the second r -process peak ($A \sim 130$). These findings suggest that the strength of the magnetic fields in CC-SNe significantly influences the extent of r -process nucleosynthesis, with only the most magnetically energetic events contributing to the production of the heaviest r -process elements.

Contemporary models suggest that the most promising CC-SNe sites for full r -process nucleosynthesis involve extreme physical conditions, such as those found in magneto-rotationally driven jets [70,85,86] and collapsar disk winds [87,88]. In these rare events, extremely rapid rotation and strong magnetic fields create the necessary neutron-rich ejecta for synthesizing heavy r -process nuclei. These models also indicate that such rare supernovae, if they occur, could generate substantial r -process yields ($0.01\text{--}0.1 M_{\odot}$) immediately following episodes of star formation, given the short lifetimes of their progenitors. Interestingly, collapsars have also been argued as prodigious producers of carbon, and may be responsible for the origin of the CEMP- r stars [89].

The interplay between the limited and main r -processes offers a compelling explanation for the observed abundance patterns in RPE metal-poor stars. If the main r -process produces second- and third-peak elements, while CC-SNe generate variable amounts of lighter r -process material, the resulting abundance patterns in metal-poor stars could reflect a mixture of these different nucleosynthetic processes. The presence of small, yet detectable, amounts of neutron-capture elements in most metal-poor stars could be attributed to ongoing chemical enrichment by CC-SNe, which contribute both light and heavy r -process material over time. Recent results from the RPA DR5 reveal that the $[\text{Mg}/\text{Eu}]$ ratio in RPE stars, for both r -I and r -II classes, systematically decreases with increasing metallicity, as shown in Figure 6. This trend suggests that europium, primarily produced by the

r-process, becomes increasingly abundant relative to magnesium, which is synthesized in CC-SNe. The observed behavior implies the emergence or growing contribution of additional *r*-process sources distinct from core-collapse supernovae as the Universe evolves and becomes more metal-rich.

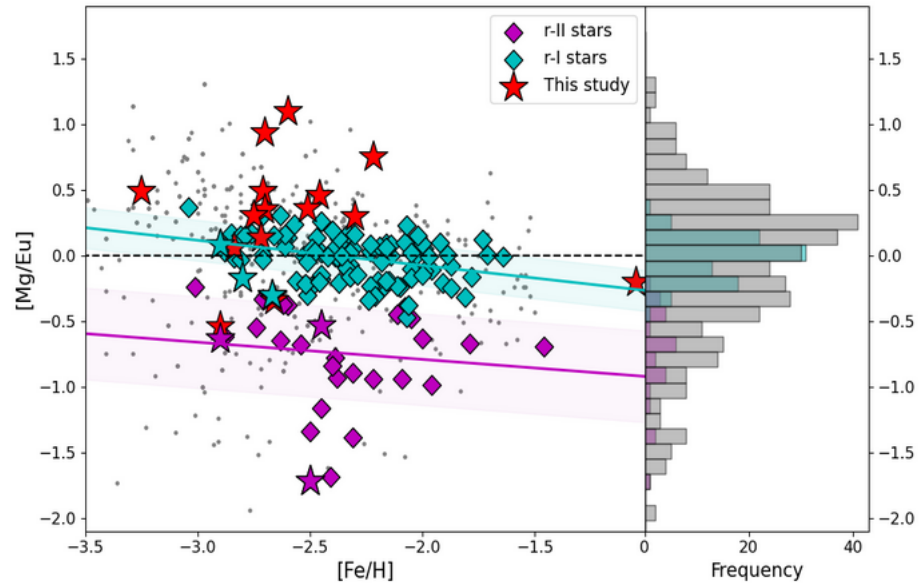


Figure 6. Distribution of $[Mg/Eu]$, as a function of $[Fe/H]$, for *r*-I, *r*-II, and non-*r*-process-enhanced (non-RPE) stars. Red stars indicate non-RPE stars, while *r*-I and *r*-II stars are taken from RPA Data Releases 1–5, with colors assigned as in the legend. Gray-filled circles represent stars from [90]. The histogram on the right compares the $[Mg/Eu]$ distributions across all metallicities. The observed downward trend of $[Mg/Eu]$ with increasing $[Fe/H]$ suggests the growing importance of a delayed nucleosynthetic source, distinct from CC-SNe that preferentially contributes europium as the Universe evolves. Figure credits: [24], reproduced with permission © AAS and was originally published in The Astrophysical Journal Supplement Series.

Interestingly, stars such as HD 122563 [79] exhibit abundance patterns that may offer a rare glimpse of a “pure” limited *r*-process signature. This metal-poor star shows a pronounced over-abundance of light neutron-capture elements relative to heavier ones, consistent with enrichment by CC-SNe ejecta that produced only first-peak *r*-process elements. However, the contribution of charged-particle reactions and *s*-process nucleosynthesis in massive stars may also play a role in shaping the abundance patterns of certain early-generation stars [91,92].

Overall, while CC-SNe are no longer considered the dominant site for the heaviest *r*-process elements [53,93], they remain important contributors to the chemical enrichment of the Galaxy, especially through their production of lighter *r*-process nuclei. The complexity of the nucleosynthesis processes, combined with the rarity of extreme explosion conditions, makes the *r*-process in CC-SNe an ongoing area of active research, with implications for the chemical evolution of galaxies and the formation of metal-poor stars.

3.3. Other Sites

As mentioned above, the *i*-process has been proposed as another source of heavy elements beyond the iron peak, up to and including the lanthanides and actinides ([26,54] and references therein). Originally suggested by [94], the discovery of CEMP stars with $[C/Fe] > +0.7$ and $[Fe/H] \leq -1.0$ exhibiting over-abundances of both *r*- and *s*-process elements (CEMP-*r/s*; see [4]) inspired models to account for this remarkable behavior. The likely astrophysical sites for the *i*-process include low-mass, low-metallicity AGB stars [26] and rapidly accreting white dwarfs ([95] and references therein). Only a few

tens of CEMP-*r/s* stars are known at present, but among those that are known, the binary fractions appear high, at least $\sim 50\%$ [96]. Definitive assignment of the astrophysical site(s) of the *i*-process awaits the discovery and high-resolution spectroscopic analysis of additional CEMP-*r/s* stars.

4. Astrophysical Environments for Studying the *r*-Process

4.1. Dwarf Galaxies

The study of *r*-process nucleosynthesis in dwarf galaxies presents unique challenges, largely due to the intrinsic faintness of their stellar populations. Dwarf galaxies, loosely defined as gravitationally bound systems of stars embedded in dark matter halos, are significantly farther away, and hence much fainter than nearby Galactic stars [97–99]. Thus, their detailed spectroscopic analysis is technically demanding. High-resolution spectroscopy of individual stars in these systems requires the use of large-aperture telescopes and long integration times, often pushing the limits of current instrumentation. Furthermore, observations in the near-UV, where several key neutron-capture element lines are located, remain infeasible for such distant and faint targets with present-day ground-based facilities.

Despite the above difficulties, dwarf galaxies offer a valuable window into the early Universe. Their relatively simpler and truncated star-formation histories preserve the chemical signatures of early nucleosynthesis events more clearly than for individual stars in the more chemically evolved Milky Way halo system. As such, they provide a unique opportunity to probe the conditions and sites responsible for the origin of heavy elements. Measurements of neutron-capture elements like strontium, barium, and europium in individual red giant stars, among the only accessible neutron-capture tracers in these systems, allow us to constrain the yields and delay times of the astrophysical events responsible for *r*-process enrichment. To date, roughly 60 dwarf galaxies are known to orbit the Milky Way [100], and they continue to serve as prime laboratories for investigating the nature of early chemical enrichment and the role of *r*-process nucleosynthesis in the broader context of galaxy evolution.

A particularly compelling case for *r*-process enrichment in dwarf galaxies emerged with the discovery of the UFD galaxy Ret II (see Figure 7). High-resolution spectroscopic observations [32–34] have revealed that the majority of its red giant stars exhibit extreme enhancements in *r*-process elements, some with europium abundance ratios exceeding $[\text{Eu}/\text{Fe}] > +1.5$ and clear signatures matching the Solar *r*-process pattern. This finding provided the first strong evidence that a single, prolific *r*-process event such as a NSM could enrich an entire dwarf galaxy in the heaviest elements. The sharp chemical imprint and the lack of a large dispersion in the *r*-process abundance patterns among the RPE stars suggest that the *r*-process material was injected into the interstellar medium rapidly and uniformly, before any significant dilution or subsequent star formation occurred.

RPE stars have also been found in other dwarfs, such as Tucana III [101] and possibly in the more massive Sculptor and Fornax dwarf galaxies [102,103], although with more complex enrichment histories. These discoveries support the idea that NSMs, despite their presumed long delay times, can occur early and contribute significantly to *r*-process enrichment even in the smallest galactic environments. They also offer critical insight into the stochastic nature of nucleosynthetic events in low-mass systems, highlighting how a single rare event can dominate the chemical evolution of an entire galaxy.

The variation in *r*-process enrichment across dwarf galaxies provides crucial constraints on the frequency and environmental dependence of *r*-process events. While systems like Ret II display extreme enhancements, many other dwarf galaxies, particularly the classical and more massive ones, exhibit only mild or negligible levels of *r*-process element enrichment. For instance, in dwarf galaxies like Draco or Ursa Minor, only a small

fraction of stars exhibit detectable europium, and the abundances often reflect more modest enrichment, possibly from multiple weaker sources or events with lower yields.

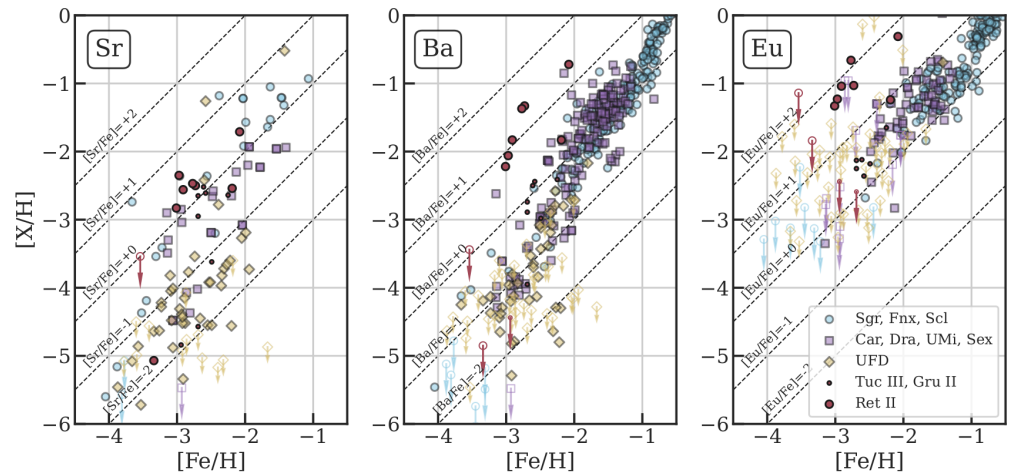


Figure 7. Neutron-capture element abundances in dwarf galaxies vary with stellar mass. In this figure, taken from [93], blue circles represent more massive classical dSphs, purple squares correspond to intermediate-mass classical dSphs, yellow diamonds mark UFDs without r -process signatures, and red circles highlight the few UFDs with r -process enhancement. Reticulum II (Ret II) is shown with larger symbols to emphasize its higher [Eu/Fe] compared to Tucana III and Grus II. Open symbols with downward arrows indicate upper limits where no detection was possible. Most UFDs have lower neutron-capture abundances than classical dSphs across $-3 < [\text{Fe}/\text{H}] < -2$, except for the rare r -process-enhanced systems. Upper limits for strontium and barium are often meaningful, while those for europium mainly reflect the difficulty of its detection at low abundances. The increase in barium at $[\text{Fe}/\text{H}] \geq -2$ among classical dSphs and some UFDs indicates the onset of significant s -process enrichment. The figure is reproduced with permission from the authors.

The wide range of enrichment levels suggests that r -process production in dwarf galaxies is not uniform but instead stochastic, likely depending on factors such as star-formation efficiency, gas retention, and the timing and/or location of explosive events. Ultra-faint dwarfs, with their limited star formation and shallow potential wells, are especially susceptible to enrichment from a single nucleosynthesis event, making them ideal laboratories to study the imprint of individual r -process progenitors. In contrast, more massive dwarfs may host a more prolonged and mixed chemical evolution, where the signal from r -process events becomes diluted or confounded with contributions from other processes. By comparing the chemical patterns across systems with different masses and star-formation histories, astronomers can begin to piece together a more complete picture of how and when the r -process shaped the early chemical evolution of galaxies [104].

4.2. Globular Clusters

Globular clusters (GCs), once regarded as simple, chemically homogeneous stellar populations that were formed in a single burst, have undergone a dramatic conceptual transformation. This shift began in the 1970s with the groundbreaking discovery of star-to-star abundance variations in light elements like carbon and nitrogen [105], followed by sodium and oxygen [106,107]. These early findings changed the classical paradigm, revealing that GCs harbor multiple stellar populations with distinct chemical fingerprints [108–110]. Spectroscopic studies, including the extensive survey by [111,112], solidified this picture, demonstrating that light-element anti-correlations (such as Na-O) are a defining feature of nearly all Galactic GCs. Complementing this, high-precision HST photometry [113–116] uncovered distinct photometric sequences corresponding to chemically distinct sub-populations, linking spec-

troscopic abundance patterns with variations in He, C, N, and O. While variations in light elements could be traced to high-temperature hydrogen burning in a previous generation of stars, the detection of inhomogeneities in heavier elements, especially those forged in the *r*-process, presented a far more profound and intriguing challenge.

The first compelling evidence for such *r*-process dispersion came from M15. Ref. [117] discovered strong star-to-star variations in Eu and Ba, with a remarkably constant [Eu/Ba] ratio pointing to a pure *r*-process origin. This suggested that a singular, potent nucleosynthetic event may have seeded the cluster with both of these elements. Follow-up studies [118–121] confirmed this picture and, crucially, demonstrated that these heavy-element anomalies were decoupled from the canonical light-element trends. In M15, stars enriched in Na and depleted in Mg bore no connection to their *r*-process content, pointing to distinct enrichment pathways.

Explaining these abundance patterns turned out to be challenging. Theories invoking neutron star mergers (NSMs) post-star formation [52,122] were undermined by observations like those of [123], who showed constant [Ba/Fe] across evolutionary stages—contradicting expectations from surface pollution. More plausible are models invoking rare, early in situ events such as magneto-rotational supernovae or NSMs that enriched the proto-cluster gas before it fully mixed [124], leaving behind localized chemical signatures in the first generation of stars. For a time, M15 stood as a lone anomaly. Ref. [125] found similar *r*-process dispersion in M92, another ancient, metal-poor cluster, with elements like Y, Zr, La, and Eu showing clear star-to-star variations. This raised the possibility that such signatures might be a common feature of the most ancient GCs. Such signatures were also found in globular cluster escapees [126]. Yet, not all studies agreed. Ref. [127], using high-resolution Keck/HIRES data, failed to confirm the M92 dispersions, highlighting the delicate interplay between data quality and astrophysical interpretation. Ref. [128] further cautioned that small systematic errors in atmospheric parameters could mimic abundance spreads.

The past two years have ushered in a resurgence of clarity. Ref. [129], for the first time, provided robust evidence for *r*-process dispersion in M92, but with a remarkable twist: the variation was largely confined to first-generation stars (low-Na and high-Mg), marking the first observed link between light-element and neutron-capture abundances in a GC. Their findings imply a localized, inhomogeneous injection of *r*-process material during the cluster's earliest formation phase, preceding the formation of second-generation stars by at least 0.8 Myr. Meanwhile, Ref. [130] presented an extensive spectroscopic study of M15, finding that a majority of its stars are either *r*-I or *r*-II stars, and confirmed significant dispersion in the neutron-capture elements from Sr to Dy. Intriguingly, they also uncovered tentative correlations between Na and *r*-process abundances—an unexpected result that hints at a more complex chemical evolution than previously thought. Adding to this, Ref. [131] analyzed NGC 2298 and found significant Sr and Eu dispersions among first-generation stars, along with correlations between [Sr/Eu], [Ba/Eu], and [Mg/Fe], suggesting a shared origin for light *r*-process elements and Mg. The cluster follows a universal *r*-process pattern, but with greater scatter for main *r*-process elements than for the limited-*r* group, highlighting multiple early enrichment pathways.

Collectively, these discoveries transformed the narrative of GCs from simple relics to dynamic archives of early cosmic nucleosynthesis. The evidence for real and intrinsic *r*-process dispersion in clusters like M15, M92, and NGC 2298 suggests that some GCs were enriched by rare, high-yield events such as NSMs or exotic supernovae, while others were not, highlighting the stochastic nature of *r*-process enrichment in the early Universe. These ancient stellar systems thus offer a powerful probe into the timing, frequency, and diversity of heavy-element production in the Galaxy's infancy. Moving forward, detailed chemical

tagging, precise abundance measurements, and next-generation simulations are essential to map the fingerprints of the earliest r -process events and their role in shaping the chemical landscape of the Milky Way.

4.3. Galactic Stars

Individual Galactic stars with over-abundances of r -process elements have been recognized for several decades (starting with [132]) and have been reported in the literature on a case-by-case basis ever since. However, until recently, there has not been a sufficiently large sample of RPE stars to make significant headway on understanding the nature of their progenitor(s). Fortunately, dedicated surveys to identify larger inventories of stars with elemental-abundance patterns associated with the r -process have been underway over the course of the past decade. These include the RPA, mentioned above, as well as detailed observations from the Chemical Evolution of R-process Elements in Stars (CERES) effort ([133] and references therein). The upcoming RPA release of the results of high-resolution spectroscopic follow-up of some 2000 metal-poor stars, expected to include numerous new limited- r , r -I, and r -II stars, will expand their numbers by roughly a factor of at least two and hopefully enable better understanding.

Observations of individual Galactic stars have clear advantages for the detailed study of the r -process, as they are significantly brighter than stars in dwarf galaxies and globular clusters and allow for the examination of main-sequence dwarfs rather than exclusively giants. This enables high-S/N spectra to be obtained, from which even weak lines of neutron-capture elements can be examined. In addition, a subset of such stars are sufficiently bright that they can be observed at high resolution in the near-UV with HST/STIS, opening pathways to include elements that do not possess lines in the optical range. The powerful combination of ground-based and space-based high-resolution observations is clearly shown by the case of the halo star HD 222925, a metal-poor star with the most complete set of abundances for any object outside the Solar System ([134]; see Figure 8).

With the advent of the Gaia mission [135], precision astrometry (geometric parallaxes and proper motions), and for brighter stars, moderate-resolution spectroscopy in the region of the Ca triplet, from which radial velocities can be obtained, have enabled the derivation of dynamical parameters for individual RPE stars. Based on this information, a growing number of studies (e.g., [136–139]) have explored the dynamical associations of such stars, tracing them back to their likely sites of origin (expected to be primarily disrupted dwarf galaxies). These so-called “chemo-dynamically tagged groups” (CDTGs) allow inferences to be made of the range of masses of their parent dwarf galaxies and provide information on their chemical-evolution histories. In this regard, it is notable that it has been recently claimed that a large fraction (at least $\sim 20\%$) of all presently recognized RPE stars in the Galactic halo might be stars that were stripped from the Ret II dwarf galaxy [140].

It is also remarkable that a few RPE stars have been identified recently at high metallicity $[\text{Fe}/\text{H}] > -1.0$, which appear to be members of the disk system of the MW [141]. These include a thin-disk star (LAMOST J020623.21+494127.9), with metallicity $[\text{Fe}/\text{H}] = -0.54$ and $[\text{Eu}/\text{Fe}] = +1.32$, that possesses the highest reported Eu to Fe ratio ($[\text{Eu}/\text{H}] = +0.78$) known. Although the study of RPE stars that are members of the disk system is still in its infancy, they have the potential to constrain its formation history, and the conditions under which RPE stars can form at high metallicity.

While nearly all current observational constraints on the r -process are based on elemental abundances, isotopic abundances, if measurable, could provide a transformative window into nucleosynthesis processes. Such data could, for example, distinguish between different r -process pathways (main vs. weak), test predictions of fission-fragment distributions, or reveal signatures of multiple enrichment events. However, measuring

isotopic abundances in stars is extremely challenging due to limited spectral resolution, blending, and the small isotopic shifts in most transitions. For a few bright Galactic stars, isotopic ratios have been measured for elements like Ba and Eu, primarily using hyperfine splitting and isotope shifts in high-resolution spectra (e.g., [142–144]). Future advances in instrumentation and modeling, especially in the infrared and UV spectra, may improve the feasibility of such measurements.

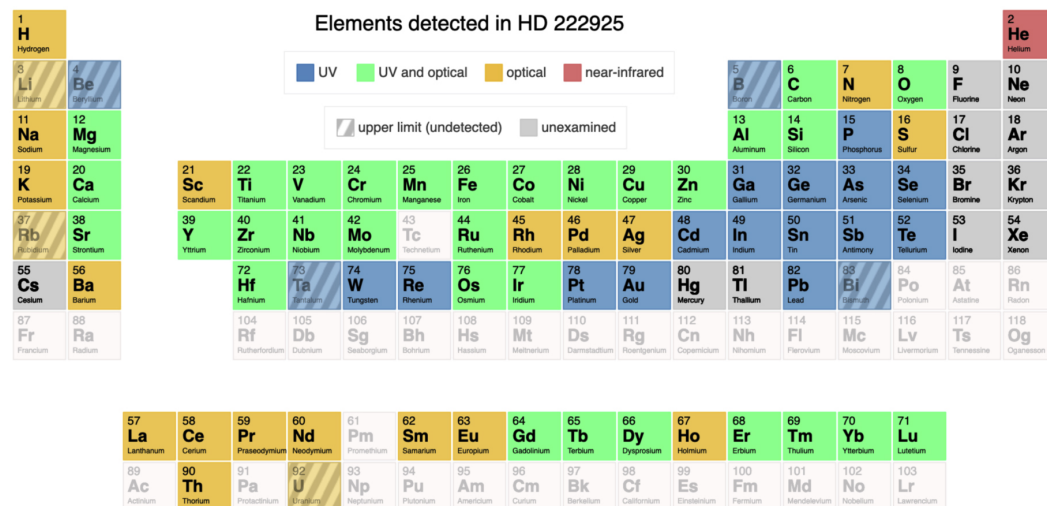


Figure 8. This figure, taken from [134], shows the elements that have been detected and measured in HD 222925 using UV and optical spectroscopy. This also illustrates the importance of UV spectroscopy to maximize the number of elements studied in a star and hence derive constraints on its production sites and progenitors. This figure is reproduced with permission © AAS and was originally published in *The Astrophysical Journal*.

5. Looking Ahead

There are a number of “mega” spectroscopic surveys now underway or planned to start in the near future. These include the Milky Way Survey within DESI [145], the 4-metre Multi-Object Spectroscopic Telescope survey (4MOST; [146]), and sub-surveys within the wide-field, massively multiplexed spectroscopic survey facility for the William Herschel Telescope (WEAVE; [147]), all of which target individual Galactic stars, at medium to high spectral resolution. The Subaru Prime Focus Spectrograph survey (PFS; [148]) will target the regions of Northern Hemisphere dwarf galaxies and of course will include foreground/background stars in their neighborhood. A high-resolution study of individual stars in Southern Hemisphere dwarf galaxies is presently being carried out with Gemini-S/GHOST. The Multi-Object Optical and Near-infrared Spectrograph (MOONS; [149]) survey on the VLT will provide moderate ($R \sim 5000$ and $R \sim 20,000$) optical and near-IR spectroscopy for stars in the Galactic Bulge, as well as in the disk system.

All of the above spectroscopic surveys will contribute to the identification of stars with over-abundances of neutron-capture elements, so we can expect significant numbers of limited- r , r -I, and r -II (as well as numerous CEMP- r , CEMP- s , and CEMP- r/s) stars to be found. The final Gaia data release, planned for roughly two years hence, will contribute hundreds of millions of additional Galactic stars with available astrometry, radial velocities, and very low-resolution spectra (the so-called XP spectra). For optimal interpretation, many of the stars identified by these surveys will need to be observed at higher resolution and/or S/N. The combination of precise astrometry and radial velocities from Gaia will enable an enormous expansion of the numbers of stars for which CDTGs can be searched, helping to constraint the nature of their birthplaces.

Given their relative rarity, the need to identify substantially larger samples of, in particular, VMP, EMP, and UMP stars in order to explore the nature of the r -process at the lowest metallicities should be given high priority. Mega photometric surveys involving narrow- and medium-band filters, mentioned below, are an ideal method to accomplish this. Over the past few years, intensive efforts have been made to refine the photometric zero-points for such surveys and for the derivation of stellar parameters and elemental abundances [150–161]. The combination of such filters with ultra-wide Gaia BP and RP photometry has been shown to provide accurate estimates of atmospheric parameters, including metallicities, and in some cases, individual elemental abundances (e.g., $[C/Fe]$, $[Mg/Fe]$, and $[\alpha/Fe]$) for stars down to about $[Fe/H] = -4.0$.

The Stellar Abundance and Galactic Evolution Survey (SAGES; [162,163]) and the SkyMapper Southern Survey (SMSS; [164,165]) efforts have been completed. The Southern Photometric Local Universe Survey (S-PLUS; [166]) and the Javalambre Photometric Local Universe Survey (J-PLUS; [167]) are ongoing and are expected to be completed in the next few years. The PRISTINE survey [11] is also ongoing. These surveys have already produced long lists of candidate EMP and UMP stars suitable for moderate-to-high-resolution follow-up, from which neutron-capture enhanced stars can be identified. The estimated numbers of VMP/EMP/UMP stars expected to be found based on the combination of the photometric surveys to date are prodigious: tens of millions of stars with $[Fe/H] \leq -2.0$, hundreds of thousands with $[Fe/H] \leq -3.0$, and several thousand stars with $[Fe/H] \leq -4.0$.

The Ultra Short Survey (USS; [168]), a sub-survey within S-PLUS, is of particular note, as it is based on substantially shorter exposure times than the normal S-PLUS program. This enables much brighter stars to be observed without saturation, including stars as bright as $G \sim 7.0$. The Javalambre Physics of the Accelerating Universe Astrophysical Survey (J-PAS; [169]), already underway, is based on over 50 narrow-to-medium-band filters over most of the optical region. Based on these data, it is expected that numerous individual elemental abundances can be estimated, possibly including several neutron-capture elements.

An auxiliary survey, the Mapping the Ancient Galaxy In CaHK (MAGIC) survey, using a narrow-band CaII HK filter in combination with observations from the already completed Dark Energy Survey, which included only broad-band filters, is underway with the Dark Energy Camera (DECam) at the 4 m Blanco Telescope (see [170]). Similar efforts in order to supplement the soon-to-begin Legacy Survey of Space and Time (LSST; see [171,172]) at the Vera C. Rubin Observatory would also be of great interest.

A major challenge in modeling r -process nucleosynthesis arises from the scarcity of experimental nuclear data for the very neutron-rich nuclei involved. Many of these isotopes lie far from stability and have extremely short half-lives, making them inaccessible to direct measurements with current accelerator facilities. As a result, key inputs such as nuclear masses, β -decay rates, neutron-capture rates, and fission yields often rely on theoretical models, which introduce significant uncertainties in the predicted abundance patterns. Efforts at next-generation radioactive ion beam facilities (e.g., FRIB, FAIR, and RIKEN) are beginning to extend the reach of experiments toward the relevant regions of the nuclear chart, but comprehensive coverage remains a long-term goal. These experimental limitations underline the need for close collaboration between nuclear theory, laboratory measurements, and astrophysical observations.

Finally, it must be acknowledged that in r -process nucleosynthesis the resulting abundance patterns are strongly influenced by the underlying nuclear physics inputs. Although r -process elements are mainly produced through rapid neutron capture and beta decay, the uncertainties due to specific reaction rates and cross sections are comparatively low under the extreme conditions of high temperature and neutron density. Instead, nu-

clear masses (which determine (n,γ) Q-values) and β -decay rates along the neutron-rich isotopic chains play a dominant role in shaping the abundance pattern and setting the timescales. Additionally, fission processes, including fission recycling, can significantly alter the production of the heaviest nuclei, particularly in very neutron-rich environments such as neutron star mergers. Recent progress in experimental and theoretical nuclear physics such as measurements of β -decay half-lives at radioactive ion beam facilities and improved global mass models has begun to refine our understanding of these processes. These nuclear properties are often uncertain and far from stability, and current experimental and theoretical efforts are helping to reduce these uncertainties as discussed in [25,173,174].

Author Contributions: Conceptualization, A.B. and T.C.B.; methodology, A.B. and T.C.B.; validation, A.B. and T.C.B.; formal analysis, A.B. and T.C.B.; investigation, A.B. and T.C.B.; resources A.B. and T.C.B.; writing—original draft preparation, A.B. and T.C.B.; writing—review and editing, A.B. and T.C.B.; visualization, A.B.; supervision, T.C.B.; project administration, A.B. and T.C.B. All authors have read and agreed to the published version of the manuscript.

Funding: T.C.B. acknowledges funding support from grant PHY 14-30152: Physics Frontier Center/JINA Center for the Evolution of the Elements (JINA-CEE), and from OISE-1927130: The International Research Network for Nuclear Astrophysics (IReNA), awarded by the US National Science Foundation.

Conflicts of Interest: The authors declare no conflicts of interest.

Notes

- ¹ Recently, the i -process has been suggested to also contribute a portion of the heaviest elements, particularly at the lowest metallicities (see [26] and references therein).
- ² Delayed β decay is the process by which unstable, neutron-rich nuclei produced during the r -process undergo β decay after neutron flux ceases, transforming into more stable elements and shaping the final abundance pattern.
- ³ $[\text{Fe}/\text{H}] = \log_{10} (N(\text{Fe})/N(\text{H}))_{\star} - \log_{10} (N(\text{Fe})/N(\text{H}))_{\odot}$, where $N(\text{Fe})$ and $N(\text{H})$ represent the number densities of iron and hydrogen, respectively. $[\text{X}/\text{Y}] = \log_{10} (N(\text{X})/N(\text{Y}))_{\star} - \log_{10} (N(\text{X})/N(\text{Y}))_{\odot}$, where $N(\text{X})$ and $N(\text{Y})$ represent the number densities of elements X and Y, respectively. For sun, $[\text{Fe}/\text{H}]_{\odot}$ is defined as zero to set a reference point or benchmark.

References

1. Beers, T.C.; Preston, G.W.; Shtetman, S.A. A search for stars of very low metal abundance. I. *Astron. J.* **1985**, *90*, 2089–2102. [\[CrossRef\]](#)
2. Beers, T.C.; Preston, G.W.; Shtetman, S.A. A search for stars of very low metal abundance. II. *Astron. J.* **1992**, *103*, 1987–2034. [\[CrossRef\]](#)
3. McWilliam, A.; Preston, G.W.; Sneden, C.; Searle, L. Spectroscopic Analysis of 33 of the Most Metal Poor Stars. II. *Astron. J.* **1995**, *109*, 2757. [\[CrossRef\]](#)
4. Beers, T.C.; Christlieb, N. The Discovery and Analysis of Very Metal-Poor Stars in the Galaxy. *Annu. Rev. Astron. Astrophys.* **2005**, *43*, 531–580. [\[CrossRef\]](#)
5. Bromm, V.; Yoshida, N.; Hernquist, L.; McKee, C.F. The formation of the first stars and galaxies. *Nature* **2009**, *459*, 49–54. [\[CrossRef\]](#)
6. Frebel, A.; Norris, J.E. Near-Field Cosmology with Extremely Metal-Poor Stars. *Annu. Rev. Astron. Astrophys.* **2015**, *53*, 631–688. [\[CrossRef\]](#)
7. Cowan, J.J.; Sneden, C.; Lawler, J.E.; Aprahamian, A.; Wiescher, M.; Langanke, K.; Martínez-Pinedo, G.; Thielemann, F.K. Origin of the heaviest elements: The rapid neutron-capture process. *Rev. Mod. Phys.* **2021**, *93*, 015002. [\[CrossRef\]](#)
8. Kobayashi, C.; Karakas, A.I.; Lugaro, M. The Origin of Elements from Carbon to Uranium. *Astrophys. J.* **2020**, *900*, 179. [\[CrossRef\]](#)
9. Schatz, H.; Reyes, A.D.B.; Best, A.; Brown, E.F.; Chatziioannou, K.; Chipps, K.A.; Deibel, C.M.; Ezzeddine, R.; Galloway, D.K.; Hansen, C.J.; et al. Horizons: Nuclear astrophysics in the 2020s and beyond. *J. Phys. G Nucl. Part. Phys.* **2022**, *49*, 110502. [\[CrossRef\]](#)
10. Christlieb, N. Finding the Most Metal-poor Stars of the Galactic Halo with the Hamburg/ESO Objective-prism Survey (with 6 Figures). *Rev. Mod. Astron.* **2003**, *16*, 191–206. [\[CrossRef\]](#)
11. Starkenburg, E.; Martin, N.; Youakim, K.; Aguado, D.S.; Allende Prieto, C.; Arentsen, A.; Bernard, E.J.; Bonifacio, P.; Caffau, E.; Carlberg, R.G.; et al. The Pristine survey—I. Mining the Galaxy for the most metal-poor stars. *Mon. Not. R. Astron. Soc.* **2017**, *471*, 2587–2604. [\[CrossRef\]](#)

12. Bandyopadhyay, A.; Sivarani, T.; Susmitha, A.; Beers, T.C.; Giridhar, S.; Surya, A.; Masseron, T. Chemical Composition of Two Bright, Extremely Metal-poor Stars from the SDSS MARVELS Pre-survey. *Astrophys. J.* **2018**, *859*, 114. [\[CrossRef\]](#)
13. Bonifacio, P.; Molaro, P.; Sivarani, T.; Cayrel, R.; Spite, M.; Spite, F.; Plez, B.; Andersen, J.; Barbuy, B.; Beers, T.C.; et al. First stars VII—Lithium in extremely metal poor dwarfs. *Astron. Astrophys.* **2007**, *462*, 851–864. [\[CrossRef\]](#)
14. Masseron, T.; Johnson, J.A.; Lucatello, S.; Karakas, A.; Plez, B.; Beers, T.C.; Christlieb, N. Lithium Abundances in Carbon-enhanced Metal-poor Stars. *Astrophys. J.* **2012**, *751*, 14. [\[CrossRef\]](#)
15. Bandyopadhyay, A.; Sivarani, T.; Beers, T.C.; Susmitha, A.; Nayak, P.K.; Pandey, J.C. Li Distribution, Kinematics, and Detailed Abundance Analysis among Very Metal-poor Stars in the Galactic Halo from the HESP-GOMPA Survey. *Astrophys. J.* **2022**, *937*, 52. [\[CrossRef\]](#)
16. Frebel, A. From Nuclei to the Cosmos: Tracing Heavy-Element Production with the Oldest Stars. *Annu. Rev. Nucl. Part. Sci.* **2018**, *68*, 237–269. [\[CrossRef\]](#)
17. Christlieb, N.; Beers, T.C.; Barklem, P.S.; Bessell, M.; Hill, V.; Holmberg, J.; Korn, A.J.; Marsteller, B.; Mashonkina, L.; Qian, Y.Z.; et al. The Hamburg/ESO R-process Enhanced Star survey (HERES). I. Project description, and discovery of two stars with strong enhancements of neutron-capture elements. *Astron. Astrophys.* **2004**, *428*, 1027–1037. [\[CrossRef\]](#)
18. Barklem, P.S.; Christlieb, N.; Beers, T.C.; Hill, V.; Bessell, M.S.; Holmberg, J.; Marsteller, B.; Rossi, S.; Zickgraf, F.J.; Reimers, D. The Hamburg/ESO R-process enhanced star survey (HERES). II. Spectroscopic analysis of the survey sample. *Astron. Astrophys.* **2005**, *439*, 129–151. [\[CrossRef\]](#)
19. Siqueira Mello, C.; Hill, V.; Barbuy, B.; Spite, M.; Spite, F.; Beers, T.C.; Caffau, E.; Bonifacio, P.; Cayrel, R.; François, P.; et al. High-resolution abundance analysis of very metal-poor r-I stars. *Astron. Astrophys.* **2014**, *565*, A93. [\[CrossRef\]](#)
20. Hansen, T.T.; Holmbeck, E.M.; Beers, T.C.; Placco, V.M.; Roederer, I.U.; Frebel, A.; Sakari, C.M.; Simon, J.D.; Thompson, I.B. The R-process Alliance: First Release from the Southern Search for R-process-enhanced Stars in the Galactic Halo. *Astrophys. J.* **2018**, *858*, 92. [\[CrossRef\]](#)
21. Sakari, C.M.; Placco, V.M.; Farrell, E.M.; Roederer, I.U.; Wallerstein, G.; Beers, T.C.; Ezzeddine, R.; Frebel, A.; Hansen, T.; Holmbeck, E.M.; et al. The R-Process Alliance: First Release from the Northern Search for r-process-enhanced Metal-poor Stars in the Galactic Halo. *Astrophys. J.* **2018**, *868*, 110. [\[CrossRef\]](#)
22. Ezzeddine, R.; Rasmussen, K.; Frebel, A.; Chiti, A.; Hinojisa, K.; Placco, V.M.; Ji, A.P.; Beers, T.C.; Hansen, T.T.; Roederer, I.U.; et al. The R-Process Alliance: First Magellan/MIKE Release from the Southern Search for R-process-enhanced Stars. *Astrophys. J.* **2020**, *898*, 150. [\[CrossRef\]](#)
23. Holmbeck, E.M.; Hansen, T.T.; Beers, T.C.; Placco, V.M.; Whitten, D.D.; Rasmussen, K.C.; Roederer, I.U.; Ezzeddine, R.; Sakari, C.M.; Frebel, A.; et al. The R-Process Alliance: Fourth Data Release from the Search for R-process-enhanced Stars in the Galactic Halo. *Astrophys. J. Suppl. Ser.* **2020**, *249*, 30. [\[CrossRef\]](#)
24. Bandyopadhyay, A.; Ezzeddine, R.; Allende Prieto, C.; Aria, N.; Shah, S.P.; Beers, T.C.; Frebel, A.; Hansen, T.T.; Holmbeck, E.M.; Placco, V.M.; et al. The R-process Alliance: Fifth Data Release from the Search for R-process-enhanced Metal-poor Stars in the Galactic Halo with the GTC. *Astrophys. J. Suppl. Ser.* **2024**, *274*, 39. [\[CrossRef\]](#)
25. Thielemann, F.K.; Eichler, M.; Panov, I.V.; Wehmeyer, B. Neutron Star Mergers and Nucleosynthesis of Heavy Elements. *Annu. Rev. Nucl. Part. Sci.* **2017**, *67*, 253–274. [\[CrossRef\]](#)
26. Choplin, A.; Siess, L.; Goriely, S.; Martinet, S. The intermediate neutron capture process. V. The i-process in AGB stars with overshoot. *Astron. Astrophys.* **2024**, *684*, A206. [\[CrossRef\]](#)
27. Abbott, B.P. et al. [LIGO Scientific Collaboration]; [Virgo Collaboration] Estimating the Contribution of Dynamical Ejecta in the Kilonova Associated with GW170817. *Astrophys. J. Lett.* **2017**, *850*, L39. [\[CrossRef\]](#)
28. Watson, D.; Hansen, C.J.; Selsing, J.; Koch, A.; Malesani, D.B.; Andersen, A.C.; Fynbo, J.P.U.; Arcones, A.; Bauswein, A.; Covino, S.; et al. Identification of strontium in the merger of two neutron stars. *Nature* **2019**, *574*, 497–500. [\[CrossRef\]](#)
29. Holmbeck, E.M.; Frebel, A.; McLaughlin, G.C.; Mumpower, M.R.; Sprouse, T.M.; Surman, R. Actinide-rich and Actinide-poor r-process-enhanced Metal-poor Stars Do Not Require Separate r-process Progenitors. *Astrophys. J.* **2019**, *881*, 5. [\[CrossRef\]](#)
30. Bandyopadhyay, A.; Sivarani, T.; Beers, T.C. Abundance Analysis of New r-process-enhanced Stars from the HESP-GOMPA Survey. *Astrophys. J.* **2020**, *899*, 22. [\[CrossRef\]](#)
31. Wanajo, S.; Fujibayashi, S.; Hayashi, K.; Kiuchi, K.; Sekiguchi, Y.; Shibata, M. Actinide-Boosting *r* Process in Black-Hole–Neutron-Star Merger Ejecta. *Phys. Rev. Lett.* **2024**, *133*, 241201. [\[CrossRef\]](#)
32. Ji, A.P.; Frebel, A.; Chiti, A.; Simon, J.D. R-process enrichment from a single event in an ancient dwarf galaxy. *Nature* **2016**, *531*, 610–613. [\[CrossRef\]](#)
33. Ji, A.P.; Frebel, A. From Actinides to Zinc: Using the Full Abundance Pattern of the Brightest Star in Reticulum II to Distinguish between Different r-process Sites. *Astrophys. J.* **2018**, *856*, 138. [\[CrossRef\]](#)
34. Ji, A.P.; Simon, J.D.; Roederer, I.U.; Magg, E.; Frebel, A.; Johnson, C.I.; Klessen, R.S.; Magg, M.; Cescutti, G.; Mateo, M.; et al. Metal Mixing in the r-process Enhanced Ultrafaint Dwarf Galaxy Reticulum II. *Astron. J.* **2023**, *165*, 100. [\[CrossRef\]](#)

35. Simmerer, J.; Sneden, C.; Cowan, J.J.; Collier, J.; Woolf, V.M.; Lawler, J.E. The Rise of the s-Process in the Galaxy. *Astrophys. J.* **2004**, *617*, 1091–1114. [\[CrossRef\]](#)
36. Sneden, C.; Cowan, J.J.; Gallino, R. Neutron-capture elements in the early galaxy. *Annu. Rev. Astron. Astrophys.* **2008**, *46*, 241–288. [\[CrossRef\]](#)
37. Hotokezaka, K.; Beniamini, P.; Piran, T. Neutron star mergers as sites of r-process nucleosynthesis and short gamma-ray bursts. *Int. J. Mod. Phys. D* **2018**, *27*, 1842005. [\[CrossRef\]](#)
38. Keller, S.C.; Bessell, M.S.; Frebel, A.; Casey, A.R.; Asplund, M.; Jacobson, H.R.; Lind, K.; Norris, J.E.; Yong, D.; Heger, A.; et al. A single low-energy, iron-poor supernova as the source of metals in the star SMSS J031300.36-670839.3. *Nature* **2014**, *506*, 463–466. [\[CrossRef\]](#)
39. Sneden, C.; Cowan, J.J.; Ivans, I.I.; Fuller, G.M.; Burles, S.; Beers, T.C.; Lawler, J.E. Evidence of Multiple R-Process Sites in the Early Galaxy: New Observations of CS 22892-052. *Astrophys. J. Lett.* **2000**, *533*, L139–L142. [\[CrossRef\]](#)
40. Cayrel, R.; Hill, V.; Beers, T.C.; Barbuy, B.; Spite, M.; Spite, F.; Plez, B.; Andersen, J.; Bonifacio, P.; François, P.; et al. Measurement of stellar age from uranium decay. *Nature* **2001**, *409*, 691–692. [\[CrossRef\]](#)
41. Frebel, A.; Johnson, J.L.; Bromm, V. Probing the formation of the first low-mass stars with stellar archaeology. *Mon. Not. R. Astron. Soc.* **2007**, *380*, L40–L44. [\[CrossRef\]](#)
42. Cain, M.; Frebel, A.; Ji, A.P.; Placco, V.M.; Ezzeddine, R.; Roederer, I.U.; Hattori, K.; Beers, T.C.; Meléndez, J.; Hansen, T.T.; et al. The R-Process Alliance: A Very Metal-poor, Extremely r-process-enhanced Star with $[\text{Eu}/\text{Fe}] = +2.2$, and the Class of r-III Stars. *Astrophys. J.* **2020**, *898*, 40. [\[CrossRef\]](#)
43. Roederer, I.U.; Beers, T.C.; Hattori, K.; Placco, V.M.; Hansen, T.T.; Ezzeddine, R.; Frebel, A.; Holmbeck, E.M.; Sakari, C.M. The R-Process Alliance: 2MASS J22132050-5137385, the Star with the Highest-known r-process Enhancement at $[\text{Eu}/\text{Fe}] = +2.45$. *Astrophys. J.* **2024**, *971*, 158. [\[CrossRef\]](#)
44. Hirai, Y.; Beers, T.C.; Lee, Y.S.; Wanajo, S.; Roederer, I.U.; Tanaka, M.; Chiba, M.; Saitoh, T.R.; Placco, V.M.; Hansen, T.T.; et al. The r-process Alliance: Enrichment of R-process Elements in a Simulated Milky Way-like Galaxy. *arXiv* **2024**, arXiv:2410.11943. [\[CrossRef\]](#)
45. Hansen, T.T.; Andersen, J.; Nordström, B.; Beers, T.C.; Yoon, J.; Buchhave, L.A. The role of binaries in the enrichment of the early Galactic halo. I. r-process-enhanced metal-poor stars. *Astron. Astrophys.* **2015**, *583*, A49. [\[CrossRef\]](#)
46. Hill, V.; Plez, B.; Cayrel, R.; Beers, T.C.; Nordström, B.; Andersen, J.; Spite, M.; Spite, F.; Barbuy, B.; Bonifacio, P.; et al. First stars. I. The extreme r-element rich, iron-poor halo giant CS 31082-001. Implications for the r-process site(s) and radioactive cosmochronology. *Astron. Astrophys.* **2002**, *387*, 560–579. [\[CrossRef\]](#)
47. Mashonkina, L.; Christlieb, N.; Eriksson, K. The Hamburg/ESO R-process Enhanced Star survey (HERES). X. HE 2252-4225, one more r-process enhanced and actinide-boost halo star. *Astron. Astrophys.* **2014**, *569*, A43. [\[CrossRef\]](#)
48. Holmbeck, E.M.; Beers, T.C.; Roederer, I.U.; Placco, V.M.; Hansen, T.T.; Sakari, C.M.; Sneden, C.; Liu, C.; Lee, Y.S.; Cowan, J.J.; et al. The R-Process Alliance: 2MASS J09544277+5246414, the Most Actinide-enhanced R-II Star Known. *Astrophys. J. Lett.* **2018**, *859*, L24. [\[CrossRef\]](#)
49. Placco, V.M.; Almeida-Fernandes, F.; Holmbeck, E.M.; Roederer, I.U.; Mardini, M.K.; Hayes, C.R.; Venn, K.; Chiboucas, K.; Deibert, E.; Gamen, R.; et al. SPLUS J142445.34-254247.1: An r-process-enhanced, Actinide-boost, Extremely Metal-poor Star Observed with GHOST. *Astrophys. J.* **2023**, *959*, 60. [\[CrossRef\]](#)
50. Roederer, I.U.; Vassh, N.; Holmbeck, E.M.; Mumpower, M.R.; Surman, R.; Cowan, J.J.; Beers, T.C.; Ezzeddine, R.; Frebel, A.; Hansen, T.T.; et al. Element abundance patterns in stars indicate fission of nuclei heavier than uranium. *Science* **2023**, *382*, 1177–1180. [\[CrossRef\]](#)
51. Thielemann, F.K.; Arcones, A.; Käppeli, R.; Liebendörfer, M.; Rauscher, T.; Winteler, C.; Fröhlich, C.; Dillmann, I.; Fischer, T.; Martinez-Pinedo, G.; et al. What are the astrophysical sites for the r-process and the production of heavy elements? *Prog. Part. Nucl. Phys.* **2011**, *66*, 346–353. [\[CrossRef\]](#)
52. Tsujimoto, T.; Shigeyama, T. The Origins of Light and Heavy R-process Elements Identified by Chemical Tagging of Metal-poor Stars. *Astrophys. J. Lett.* **2014**, *795*, L18. [\[CrossRef\]](#)
53. Bandyopadhyay, A.; Beers, T.C.; Ezzeddine, R.; Sivarani, T.; Nayak, P.K.; Pandey, J.C.; Saraf, P.; Susmitha, A. A chemodynamical analysis of bright metal-poor stars from the HESP-GOMPA survey—Indications of a non-prevailing site for light r-process elements. *Mon. Not. R. Astron. Soc.* **2024**, *529*, 2191–2207. [\[CrossRef\]](#)
54. Hampel, M.; Karakas, A.I.; Stancliffe, R.J.; Meyer, B.S.; Lugaro, M. Learning about the Intermediate Neutron-capture Process from Lead Abundances*. *Astrophys. J.* **2019**, *887*, 11. [\[CrossRef\]](#)
55. Drout, M.R.; Piro, A.L.; Shappee, B.J.; Kilpatrick, C.D.; Simon, J.D.; Contreras, C.; Coulter, D.A.; Foley, R.J.; Siebert, M.R.; Morrell, N.; et al. Light curves of the neutron star merger GW170817/SSS17a: Implications for r-process nucleosynthesis. *Science* **2017**, *358*, 1570–1574. [\[CrossRef\]](#) [\[PubMed\]](#)
56. Perego, A.; Radice, D.; Bernuzzi, S. AT 2017gfo: An Anisotropic and Three-component Kilonova Counterpart of GW170817. *Astrophys. J. Lett.* **2017**, *850*, L37. [\[CrossRef\]](#)

57. Shappee, B.J.; Simon, J.D.; Drout, M.R.; Piro, A.L.; Morrell, N.; Prieto, J.L.; Kasen, D.; Holoien, T.W.S.; Kollmeier, J.A.; Kelson, D.D.; et al. Early spectra of the gravitational wave source GW170817: Evolution of a neutron star merger. *Science* **2017**, *358*, 1574–1578. [\[CrossRef\]](#)
58. Holmbeck, E.M.; Andrews, J.J. Total r-process Yields of Milky Way Neutron Star Mergers. *Astrophys. J.* **2024**, *963*, 110. [\[CrossRef\]](#)
59. Siegel, D.M.; Metzger, B.D. Three-Dimensional General-Relativistic Magnetohydrodynamic Simulations of Remnant Accretion Disks from Neutron Star Mergers: Outflows and r-Process Nucleosynthesis. *Phys. Rev. Lett.* **2017**, *119*, 231102. [\[CrossRef\]](#)
60. Wehmeyer, B.; Fröhlich, C.; Côté, B.; Pignatari, M.; Thielemann, F.K. Using failed supernovae to constrain the Galactic r-process element production. *Mon. Not. R. Astron. Soc.* **2019**, *487*, 1745–1753. [\[CrossRef\]](#)
61. Roberts, L.F.; Lippuner, J.; Duez, M.D.; Faber, J.A.; Foucart, F.; Lombardi, J.C., Jr.; Ning, S.; Ott, C.D.; Ponce, M. The influence of neutrinos on r-process nucleosynthesis in the ejecta of black hole-neutron star mergers. *Mon. Not. R. Astron. Soc.* **2017**, *464*, 3907–3919. [\[CrossRef\]](#)
62. Ishimaru, Y.; Wanajo, S.; Prantzos, N. Neutron Star Mergers as the Origin of r-process Elements in the Galactic Halo Based on the Sub-halo Clustering Scenario. *Astrophys. J. Lett.* **2015**, *804*, L35. [\[CrossRef\]](#)
63. Maoz, D.; Nakar, E. The Neutron Star Merger Delay-time Distribution, R-process “Knees,” and the Metal Budget of the Galaxy. *Astrophys. J.* **2025**, *982*, 179. [\[CrossRef\]](#)
64. Kobayashi, C.; Mandel, I.; Belczynski, K.; Goriely, S.; Janka, T.H.; Just, O.; Ruiter, A.J.; Vanbeveren, D.; Kruckow, M.U.; Briel, M.M.; et al. Can Neutron Star Mergers Alone Explain the r-process Enrichment of the Milky Way? *Astrophys. J. Lett.* **2023**, *943*, L12. [\[CrossRef\]](#)
65. Levan, A.J.; Gompertz, B.P.; Salafia, O.S.; Bulla, M.; Burns, E.; Hotokezaka, K.; Izzo, L.; Lamb, G.P.; Malesani, D.B.; Oates, S.R.; et al. Heavy-element production in a compact object merger observed by JWST. *Nature* **2024**, *626*, 737–741. [\[CrossRef\]](#)
66. Chen, M.H.; Li, L.X.; Chen, Q.H.; Hu, R.C.; Liang, E.W. Neutron star mergers as the dominant contributor to the production of heavy r-process elements. *Mon. Not. R. Astron. Soc.* **2024**, *529*, 1154–1160. [\[CrossRef\]](#)
67. Burbidge, E.M.; Burbidge, G.R.; Fowler, W.A.; Hoyle, F. Synthesis of the Elements in Stars. *Rev. Mod. Phys.* **1957**, *29*, 547–650. [\[CrossRef\]](#)
68. Cameron, A.G.W. Nuclear Reactions in Stars and Nucleogenesis. *Publ. Astron. Soc. Pac.* **1957**, *69*, 201. [\[CrossRef\]](#)
69. McWilliam, A. Barium Abundances in Extremely Metal-poor Stars. *Astron. J.* **1998**, *115*, 1640–1647. [\[CrossRef\]](#)
70. Nishimura, N.; Takiwaki, T.; Thielemann, F.K. The r-process Nucleosynthesis in the Various Jet-like Explosions of Magnetorotational Core-collapse Supernovae. *Astrophys. J.* **2015**, *810*, 109. [\[CrossRef\]](#)
71. Shibagaki, S.; Kajino, T.; Mathews, G.J.; Chiba, S.; Nishimura, S.; Lorusso, G. Relative Contributions of the Weak, Main, and Fission-recycling r-process. *Astrophys. J.* **2016**, *816*, 79. [\[CrossRef\]](#)
72. Nishimura, N.; Sawai, H.; Takiwaki, T.; Yamada, S.; Thielemann, F.K. The Intermediate r-process in Core-collapse Supernovae Driven by the Magneto-rotational Instability. *Astrophys. J. Lett.* **2017**, *836*, L21. [\[CrossRef\]](#)
73. Nevins, B.; Roberts, L.F. Proto-neutron star convection and the neutrino-driven wind: Implications for the r-process. *Mon. Not. R. Astron. Soc.* **2023**, *520*, 3986–3999. [\[CrossRef\]](#)
74. Jones, S.; Röpke, F.K.; Fryer, C.; Ruiter, A.J.; Seitenzahl, I.R.; Nittler, L.R.; Ohlmann, S.T.; Reifarth, R.; Pignatari, M.; Belczynski, K. Remnants and ejecta of thermonuclear electron-capture supernovae—Constraining oxygen-neon deflagrations in high-density white dwarfs. *Astron. Astrophys.* **2019**, *622*, A74. [\[CrossRef\]](#)
75. Jones, S.; Röpke, F.K.; Pakmor, R.; Seitenzahl, I.R.; Ohlmann, S.T.; Edelmann, P.V.F. Do electron-capture supernovae make neutron stars?—First multidimensional hydrodynamic simulations of the oxygen deflagration. *Astron. Astrophys.* **2016**, *593*, A72. [\[CrossRef\]](#)
76. Farouqi, K.; Thielemann, F.-K.; Rosswog, S.; Kratz, K.-L. Correlations of r-process elements in very metal-poor stars as clues to their nucleosynthesis sites. *Astron. Astrophys.* **2022**, *663*, A70. [\[CrossRef\]](#)
77. Zha, S.; O’Connor, E.P.; Couch, S.M.; Leung, S.C.; Nomoto, K. Hydrodynamic simulations of electron-capture supernovae: Progenitor and dimension dependence. *Mon. Not. R. Astron. Soc.* **2022**, *513*, 1317–1328. [\[CrossRef\]](#)
78. Sneden, C.; Parthasarathy, M. The r- and s- process nuclei in the early history of the galaxy: HD 122563. *Astrophys. J.* **1983**, *267*, 757–778. [\[CrossRef\]](#)
79. Honda, S.; Aoki, W.; Ishimaru, Y.; Wanajo, S.; Ryan, S.G. Neutron-Capture Elements in the Very Metal Poor Star HD 122563. *Astrophys. J.* **2006**, *643*, 1180–1189. [\[CrossRef\]](#)
80. Xylakis-Dornbusch, T.; Hansen, T.T.; Beers, T.C.; Christlieb, N.; Ezzeddine, R.; Frebel, A.; Holmbeck, E.; Placco, V.M.; Roederer, I.U.; Sakari, C.M.; et al. The R-Process Alliance: Analysis of limited-r stars. *Astron. Astrophys.* **2024**, *688*, A123. [\[CrossRef\]](#)
81. Casey, A.R.; Schlaufman, K.C. The Universality of the Rapid Neutron-capture Process Revealed by a Possible Disrupted Dwarf Galaxy Star. *Astrophys. J.* **2017**, *850*, 179. [\[CrossRef\]](#)
82. Arcones, A.; Montes, F. Production of Light-element Primary Process Nuclei in Neutrino-driven Winds. *Astrophys. J.* **2011**, *731*, 5. [\[CrossRef\]](#)

83. Mumpower, M.R.; Jaffke, P.; Verriere, M.; Randrup, J. Primary fission fragment mass yields across the chart of nuclides. *Phys. Rev. C* **2020**, *101*, 054607. [\[CrossRef\]](#)
84. Wang, T.; Burrows, A. Supernova Explosions of the Lowest-mass Massive Star Progenitors. *Astrophys. J.* **2024**, *969*, 74. [\[CrossRef\]](#)
85. Reichert, M.; Obergaulinger, M.; Aloy, M.Á.; Gabler, M.; Arcones, A.; Thielemann, F.K. Magnetorotational supernovae: A nucleosynthetic analysis of sophisticated 3D models. *Mon. Not. R. Astron. Soc.* **2023**, *518*, 1557–1583. [\[CrossRef\]](#)
86. Zha, S.; Müller, B.; Powell, J. Nucleosynthesis in the Innermost Ejecta of Magnetorotational Supernova Explosions in Three Dimensions. *Astrophys. J.* **2024**, *969*, 141. [\[CrossRef\]](#)
87. Miller, J.M.; Sprouse, T.M.; Fryer, C.L.; Ryan, B.R.; Dolence, J.C.; Mumpower, M.R.; Surman, R. Full Transport General Relativistic Radiation Magnetohydrodynamics for Nucleosynthesis in Collapsars. *Astrophys. J.* **2020**, *902*, 66. [\[CrossRef\]](#)
88. Barnes, J.; Metzger, B.D. Signatures of r-process Enrichment in Supernovae from Collapsars. *Astrophys. J. Lett.* **2022**, *939*, L29. [\[CrossRef\]](#)
89. Siegel, D.M.; Barnes, J.; Metzger, B.D. Collapsars as a major source of r-process elements. *Nature* **2019**, *569*, 241–244. [\[CrossRef\]](#)
90. Abohalima, A.; Frebel, A. JINAbase—A Database for Chemical Abundances of Metal-poor Stars. *Astrophys. J. Suppl. Ser.* **2018**, *238*, 36. [\[CrossRef\]](#)
91. Cescutti, G.; Chiappini, C.; Hirschi, R.; Meynet, G.; Frischknecht, U. The s-process in the Galactic halo: The fifth signature of spinstars in the early Universe? *Astron. Astrophys.* **2013**, *553*, A51. [\[CrossRef\]](#)
92. Prantzos, N.; Abia, C.; Limongi, M.; Chieffi, A.; Cristallo, S. Chemical evolution with rotating massive star yields—I. The solar neighbourhood and the s-process elements. *Mon. Not. R. Astron. Soc.* **2018**, *476*, 3432–3459. [\[CrossRef\]](#)
93. Frebel, A.; Ji, A.P. Observations of R-Process Stars in the Milky Way and Dwarf Galaxies. *arXiv* **2023**, arXiv:2302.09188. [\[CrossRef\]](#)
94. Cowan, J.J.; Rose, W.K. Production of C-14 and neutrons in red giants. *Astrophys. J.* **1977**, *212*, 149–158. [\[CrossRef\]](#)
95. Denissenkov, P.A.; Herwig, F.; Woodward, P.; Androssy, R.; Pignatari, M.; Jones, S. The i-process yields of rapidly accreting white dwarfs from multicycle He-shell flash stellar evolution models with mixing parametrizations from 3D hydrodynamics simulations. *Mon. Not. R. Astron. Soc.* **2019**, *488*, 4258–4270. [\[CrossRef\]](#)
96. Yoon, J.; Beers, T.C.; Placco, V.M.; Rasmussen, K.C.; Carollo, D.; He, S.; Hansen, T.T.; Roederer, I.U.; Zeanah, J. Observational Constraints on First-star Nucleosynthesis. I. Evidence for Multiple Progenitors of CEMP-No Stars. *Astrophys. J.* **2016**, *833*, 20. [\[CrossRef\]](#)
97. McConnachie, A.W. The Observed Properties of Dwarf Galaxies in and around the Local Group. *Astron. J.* **2012**, *144*, 4. [\[CrossRef\]](#)
98. Simon, J.D. The Faintest Dwarf Galaxies. *Annu. Rev. Astron. Astrophys.* **2019**, *57*, 375–415. [\[CrossRef\]](#)
99. McConnachie, A.W.; Venn, K.A. Revised and New Proper Motions for Confirmed and Candidate Milky Way Dwarf Galaxies. *Astron. J.* **2020**, *160*, 124. [\[CrossRef\]](#)
100. Drlica-Wagner, A.; Bechtol, K.; Mau, S.; McNanna, M.; Nadler, E.O.; Pace, A.B.; Li, T.S.; Pieres, A.; Rozo, E.; Simon, J.D.; et al. Milky Way Satellite Census. I. The Observational Selection Function for Milky Way Satellites in DES Y3 and Pan-STARRS DR1. *Astrophys. J.* **2020**, *893*, 47. [\[CrossRef\]](#)
101. Marshall, J.L.; Hansen, T.; Simon, J.D.; Li, T.S.; Bernstein, R.A.; Kuehn, K.; Pace, A.B.; DePoy, D.L.; Palmese, A.; Pieres, A.; et al. Chemical Abundance Analysis of Tucana III, the Second r-process Enhanced Ultra-faint Dwarf Galaxy. *Astrophys. J.* **2019**, *882*, 177. [\[CrossRef\]](#)
102. Reichert, M.; Hansen, C.J.; Arcones, A. Extreme r-process Enhanced Stars at High Metallicity in Fornax*. *Astrophys. J.* **2021**, *912*, 157. [\[CrossRef\]](#)
103. Lucchesi, R.; Jablonka, P.; Skúladóttir, Á.; Lardo, C.; Mashonkina, L.; Primas, F.; Venn, K.; Hill, V.; Minniti, D. Extremely metal-poor stars in the Fornax and Carina dwarf spheroidal galaxies. *Astron. Astrophys.* **2024**, *686*, A266. [\[CrossRef\]](#)
104. Hirai, Y.; Saitoh, T.R.; Fujii, M.S.; Kaneko, K.; Beers, T.C. SIRIUS: Identifying Metal-poor Stars Enriched by a Single Supernova in a Dwarf Galaxy Cosmological Zoom-in Simulation Resolving Individual Massive Stars. *Astrophys. J. Lett.* **2025**, *980*, L25. [\[CrossRef\]](#)
105. Kraft, R.P. On the nonhomogeneity of metal abundances in stars of globular clusters and satellite subsystems of the Galaxy. *Annu. Rev. Astron. Astrophys.* **1979**, *17*, 309–343. [\[CrossRef\]](#)
106. Peterson, R.C. Evidence from sodium-abundance variations among red giants of M13 for inhomogeneities in the protocluster gas. *Astrophys. J. Lett.* **1980**, *237*, L87–L91. [\[CrossRef\]](#)
107. Kraft, R.P.; Sneden, C.; Smith, G.H.; Shetrone, M.D.; Langer, G.E.; Pilachowski, C.A. Proton Capture Chains in Globular Cluster Stars. II. Oxygen, Sodium, Magnesium, and Aluminum Abundances in M13 Giants Brighter Than the Horizontal Branch. *Astron. J.* **1997**, *113*, 279. [\[CrossRef\]](#)
108. Gratton, R.; Sneden, C.; Carretta, E. Abundance Variations Within Globular Clusters. *Annu. Rev. Astron. Astrophys.* **2004**, *42*, 385–440. [\[CrossRef\]](#)
109. Gratton, R.G.; Carretta, E.; Bragaglia, A. Multiple populations in globular clusters. Lessons learned from the Milky Way globular clusters. *Astron. Astrophys. Rev.* **2012**, *20*, 50. [\[CrossRef\]](#)
110. Gratton, R.; Bragaglia, A.; Carretta, E.; D’Orazi, V.; Lucatello, S.; Sollima, A. What is a globular cluster? An observational perspective. *Astron. Astrophys. Rev.* **2019**, *27*, 8. [\[CrossRef\]](#)

111. Carretta, E.; Bragaglia, A.; Gratton, R.; Lucatello, S. Na-O anticorrelation and HB. VIII. Proton-capture elements and metallicities in 17 globular clusters from UVES spectra. *Astron. Astrophys.* **2009**, *505*, 139–155. [\[CrossRef\]](#)
112. Carretta, E.; Bragaglia, A.; Gratton, R.G.; Lucatello, S.; Catanzaro, G.; Leone, F.; Bellazzini, M.; Claudi, R.; D’Orazi, V.; Momany, Y.; et al. Na-O anticorrelation and HB. VII. The chemical composition of first and second-generation stars in 15 globular clusters from GIRAFFE spectra. *Astron. Astrophys.* **2009**, *505*, 117–138. [\[CrossRef\]](#)
113. Piotto, G. Observations of multiple populations in star clusters. In *Proceedings of the International Astronomical Union, Volume 4, Symposium S258: The Ages of Stars*; Mamajek, E.E., Soderblom, D.R., Wyse, R.F.G., Eds.; Cambridge University Press: Cambridge, UK, 2009; Volume 258, pp. 233–244. [\[CrossRef\]](#)
114. Milone, A.P.; Piotto, G.; Renzini, A.; Marino, A.F.; Bedin, L.R.; Vesperini, E.; D’Antona, F.; Nardiello, D.; Anderson, J.; King, I.R.; et al. The Hubble Space Telescope UV Legacy Survey of Galactic globular clusters—IX. The Atlas of multiple stellar populations. *Mon. Not. R. Astron. Soc.* **2017**, *464*, 3636–3656. [\[CrossRef\]](#)
115. Milone, A.P.; Marino, A.F.; Da Costa, G.S.; Lagioia, E.P.; D’Antona, F.; Goudfrooij, P.; Jerjen, H.; Massari, D.; Renzini, A.; Yong, D.; et al. Multiple populations in globular clusters and their parent galaxies. *Mon. Not. R. Astron. Soc.* **2019**, *491*, 515–531. [\[CrossRef\]](#)
116. Milone, A.P.; Marino, A.F. Multiple Populations in Star Clusters. *Universe* **2022**, *8*, 359. [\[CrossRef\]](#)
117. Sneden, C.; Kraft, R.P.; Shetrone, M.D.; Smith, G.H.; Langer, G.E.; Prosser, C.F. Star-To-Star Abundance Variations Among Bright Giants in the Metal-Poor Globular Cluster M15. *Astron. J.* **1997**, *114*, 1964. [\[CrossRef\]](#)
118. Sneden, C.; Johnson, J.; Kraft, R.P.; Smith, G.H.; Cowan, J.J.; Bolte, M.S. Neutron-Capture Element Abundances in the Globular Cluster M15. *Astrophys. J. Lett.* **2000**, *536*, L85–L88. [\[CrossRef\]](#)
119. Otsuki, K.; Honda, S.; Aoki, W.; Kajino, T.; Mathews, G.J. Neutron-Capture Elements in the Metal-poor Globular Cluster M15. *Astrophys. J. Lett.* **2006**, *641*, L117–L120. [\[CrossRef\]](#)
120. Sobeck, J.S.; Kraft, R.P.; Sneden, C.; Preston, G.W.; Cowan, J.J.; Smith, G.H.; Thompson, I.B.; Shectman, S.A.; Burley, G.S. The Abundances of Neutron-capture Species in the Very Metal-poor Globular Cluster M15: A Uniform Analysis of Red Giant Branch and Red Horizontal Branch Stars. *Astron. J.* **2011**, *141*, 175. [\[CrossRef\]](#)
121. Worley, C.C.; Hill, V.; Sobeck, J.; Carretta, E. Ba and Eu abundances in M 15 giant stars. *Astron. Astrophys.* **2013**, *553*, A47. [\[CrossRef\]](#)
122. Tsujimoto, T.; Shigezawa, T. Enrichment history of r-process elements shaped by a merger of neutron star pairs. *Astron. Astrophys.* **2014**, *565*, L5. [\[CrossRef\]](#)
123. Kirby, E.N.; Duggan, G.; Ramirez-Ruiz, E.; Macias, P. The Stars in M15 Were Born with the r-process. *Astrophys. J. Lett.* **2020**, *891*, L13. [\[CrossRef\]](#)
124. Tarumi, Y.; Yoshida, N.; Inoue, S. Internal R-process Abundance Spread of M15 and a Single Stellar Population Model. *Astrophys. J. Lett.* **2021**, *921*, L11. [\[CrossRef\]](#)
125. Roederer, I.U.; Sneden, C. Heavy-element Dispersion in the Metal-poor Globular Cluster M92. *Astron. J.* **2011**, *142*, 22. [\[CrossRef\]](#)
126. Bandyopadhyay, A.; Thirupathi, S.; Beers, T.C.; Susmitha, A. A high-resolution spectroscopic study of two new Na- and Al-rich field giants—likely globular cluster escapees in the Galactic halo. *Mon. Not. R. Astron. Soc.* **2020**, *494*, 36–43. [\[CrossRef\]](#)
127. Cohen, J.G. No Heavy-element Dispersion in the Globular Cluster M92. *Astrophys. J. Lett.* **2011**, *740*, L38. [\[CrossRef\]](#)
128. Roederer, I.U.; Thompson, I.B. Detailed abundances of 15 stars in the metal-poor globular cluster NGC 4833. *Mon. Not. R. Astron. Soc.* **2015**, *449*, 3889–3910. [\[CrossRef\]](#)
129. Kirby, E.N.; Ji, A.P.; Kovalev, M. r-process Abundance Patterns in the Globular Cluster M92. *Astrophys. J.* **2023**, *958*, 45. [\[CrossRef\]](#)
130. Cabrera Garcia, J.; Sakari, C.M.; Roederer, I.U.; Evans, D.W.; Silva, P.; Mateo, M.; Song, Y.Y.; Kremin, A.; Bailey, J.I.; Walker, M.G. Abundances of Neutron-capture Elements in 62 Stars in the Globular Cluster Messier 15. *Astrophys. J.* **2024**, *967*, 101. [\[CrossRef\]](#)
131. Bandyopadhyay, A.; Ezzeddine, R.; Placco, V.M.; Frebel, A.; Aguado, D.S.; Roederer, I.U. Probing Abundance Variations among Multiple Stellar Populations in the Metal-Poor Globular Cluster NGC 2298 using Gemini-South/GHOST. *Astron. J.* **2025**, *170*, 37. [\[CrossRef\]](#)
132. Griffin, R.; Griffin, R.; Gustafsson, B.; Vieira, T. HD 115444—A Barium star of extreme population II. *Mon. Not. R. Astron. Soc.* **1982**, *198*, 637–658. [\[CrossRef\]](#)
133. Alencastro Puls, A.; Kuske, J.; Hansen, C.J.; Lombardo, L.; Visentin, G.; Arcones, A.; Fernandes de Melo, R.; Reichert, M.; Bonifacio, P.; Caffau, E.; et al. Chemical Evolution of R-process Elements in Stars (CERES): IV. An observational run-up of the third r-process peak with Hf, Os, Ir, and Pt. *Astron. Astrophys.* **2025**, *693*, A294. [\[CrossRef\]](#)
134. Roederer, I.U.; Lawler, J.E.; Den Hartog, E.A.; Placco, V.M.; Surman, R.; Beers, T.C.; Ezzeddine, R.; Frebel, A.; Hansen, T.T.; Hattori, K.; et al. The R-process Alliance: A Nearly Complete R-process Abundance Template Derived from Ultraviolet Spectroscopy of the R-process-enhanced Metal-poor Star HD 222925. *Astrophys. J. Suppl. Ser.* **2022**, *260*, 27. [\[CrossRef\]](#)
135. Gaia Collaboration; Prusti, T.; de Bruijne, J.H.J.; Brown, A.G.A.; Vallenari, A.; Babusiaux, C.; Bailer-Jones, C.A.L.; Bastian, U.; Biermann, M.; Evans, D.W.; et al. The Gaia mission. *Astron. Astrophys.* **2016**, *595*, A1. [\[CrossRef\]](#)
136. Roederer, I.U.; Hattori, K.; Valluri, M. Kinematics of Highly r-process-enhanced Field Stars: Evidence for an Accretion Origin and Detection of Several Groups from Disrupted Satellites. *Astron. J.* **2018**, *156*, 179. [\[CrossRef\]](#)

137. Gudín, D.; Shank, D.; Beers, T.C.; Yuan, Z.; Limberg, G.; Roederer, I.U.; Placco, V.; Holmbeck, E.M.; Dietz, S.; Rasmussen, K.C.; et al. The R-Process Alliance: Chemodynamically Tagged Groups of Halo r-process-enhanced Stars Reveal a Shared Chemical-evolution History. *Astrophys. J.* **2021**, *908*, 79. [\[CrossRef\]](#)
138. Hattori, K.; Okuno, A.; Roederer, I.U. Finding r-II Sibling Stars in the Milky Way with the Greedy Optimistic Clustering Algorithm. *Astrophys. J.* **2023**, *946*, 48. [\[CrossRef\]](#)
139. Shank, D.; Beers, T.C.; Placco, V.M.; Gudín, D.; Catapano, T.; Holmbeck, E.M.; Ezzeddine, R.; Roederer, I.U.; Sakari, C.M.; Frebel, A.; et al. The R-Process Alliance: Chemodynamically Tagged Groups. II. An Extended Sample of Halo r-process-enhanced Stars. *Astrophys. J.* **2023**, *943*, 23. [\[CrossRef\]](#)
140. Berczik, P.; Ishchenko, M.; Sobodar, O.; Mardini, M. Cosmological insights into the early accretion of r-process-enhanced stars: II. Dynamical identification of lost members of Reticulum II. *Astron. Astrophys.* **2024**, *692*, A130. [\[CrossRef\]](#)
141. Xie, X.J.; Shi, J.; Yan, H.L.; Chen, T.Y.; Allende Prieto, C.; Beers, T.C.; Liu, S.; Li, C.Q.; Ding, M.Y.; Tang, Y.J.; et al. Discovery of an Extremely r-process-enhanced Thin-disk Star with $[\text{Eu}/\text{H}] = +0.78$. *Astrophys. J. Lett.* **2024**, *970*, L30. [\[CrossRef\]](#)
142. Sneden, C.; Cowan, J.J.; Lawler, J.E.; Burles, S.; Beers, T.C.; Fuller, G.M. Europium Isotopic Abundances in Very Metal Poor Stars. *Astrophys. J. Lett.* **2002**, *566*, L25–L28. [\[CrossRef\]](#)
143. Aoki, W.; Honda, S.; Beers, T.C.; Sneden, C. Measurement of the Europium Isotope Ratio for the Extremely Metal poor, r-Process-enhanced Star CS 31082-001. *Astrophys. J.* **2003**, *586*, 506–511. [\[CrossRef\]](#)
144. Gallagher, A.J.; Ryan, S.G.; Hosford, A.; García Pérez, A.E.; Aoki, W.; Honda, S. The barium isotopic fractions in five metal-poor stars. *Astron. Astrophys.* **2012**, *538*, A118. [\[CrossRef\]](#)
145. Cooper, A.P.; Koposov, S.E.; Allende Prieto, C.; Manser, C.J.; Kizhuprakkat, N.; Myers, A.D.; Dey, A.; Gänsicke, B.T.; Li, T.S.; Rockosi, C.; et al. Overview of the DESI Milky Way Survey. *Astrophys. J.* **2023**, *947*, 37. [\[CrossRef\]](#)
146. de Jong, R.S.; Agertz, O.; Berbel, A.A.; Aird, J.; Alexander, D.A.; Amarsi, A.; Anders, F.; Andrae, R.; Ansarinejad, B.; Ansorge, W.; et al. 4MOST: Project overview and information for the First Call for Proposals. *Messenger* **2019**, *175*, 3–11. [\[CrossRef\]](#)
147. Jin, S.; Trager, S.C.; Dalton, G.B.; Aguerri, J.A.L.; Drew, J.E.; Falcón-Barroso, J.; Gänsicke, B.T.; Hill, V.; Iovino, A.; Pieri, M.M.; et al. The wide-field, multiplexed, spectroscopic facility WEAVE: Survey design, overview, and simulated implementation. *Mon. Not. R. Astron. Soc.* **2024**, *530*, 2688–2730. [\[CrossRef\]](#)
148. Takada, M.; Ellis, R.S.; Chiba, M.; Greene, J.E.; Aihara, H.; Arimoto, N.; Bundy, K.; Cohen, J.; Doré, O.; Graves, G.; et al. Extragalactic science, cosmology, and Galactic archaeology with the Subaru Prime Focus Spectrograph. *Publ. Astron. Soc. Jpn.* **2014**, *66*, R1. [\[CrossRef\]](#)
149. Gonzalez, O.A.; Mucciarelli, A.; Origlia, L.; Schultheis, M.; Caffau, E.; Di Matteo, P.; Randich, S.; Recio-Blanco, A.; Zoccali, M.; Bonifacio, P.; et al. MOONS Surveys of the Milky Way and its Satellites. *Messenger* **2020**, *180*, 18–23. [\[CrossRef\]](#)
150. Huang, Y.; Yuan, H.; Li, C.; Wolf, C.; Onken, C.A.; Beers, T.C.; Casagrande, L.; Mackey, D.; Da Costa, G.S.; Bland-Hawthorn, J.; et al. Milky Way Tomography with the SkyMapper Southern Survey. II. Photometric Recalibration of SMSS DR2. *Astrophys. J.* **2021**, *907*, 68. [\[CrossRef\]](#)
151. Huang, Y.; Beers, T.C.; Wolf, C.; Lee, Y.S.; Onken, C.A.; Yuan, H.; Shank, D.; Zhang, H.; Wang, C.; Shi, J.; et al. Beyond Spectroscopy. I. Metallicities, Distances, and Age Estimates for Over 20 Million Stars from SMSS DR2 and Gaia EDR3. *Astrophys. J.* **2022**, *925*, 164. [\[CrossRef\]](#)
152. Xu, S.; Yuan, H.; Niu, Z.; Yang, L.; Beers, T.C.; Huang, Y. Stellar Loci. V. Photometric Metallicities of 27 Million FGK Stars Based on Gaia Early Data Release 3. *Astrophys. J. Suppl. Ser.* **2022**, *258*, 44. [\[CrossRef\]](#)
153. Yang, L.; Yuan, H.; Xiang, M.; Duan, F.; Huang, Y.; Liu, J.; Beers, T.C.; Galarza, C.A.; Daflon, S.; Fernández-Ontiveros, J.A.; et al. J-PLUS: Stellar parameters, C, N, Mg, Ca, and $[\alpha/\text{Fe}]$ abundances for two million stars from DR1. *Astron. Astrophys.* **2022**, *659*, A181. [\[CrossRef\]](#)
154. Huang, Y.; Beers, T.C.; Yuan, H.; Tan, K.F.; Wang, W.; Zheng, J.; Li, C.; Lee, Y.S.; Li, H.N.; Zhao, J.K.; et al. Beyond Spectroscopy. II. Stellar Parameters for over 20 Million Stars in the Northern Sky from SAGES DR1 and Gaia DR3. *Astrophys. J.* **2023**, *957*, 65. [\[CrossRef\]](#)
155. Xiao, K.; Yuan, H.; López-Sanjuan, C.; Huang, Y.; Huang, B.; Beers, T.C.; Xu, S.; Wang, Y.; Yang, L.; Alcaniz, J.; et al. J-PLUS: Photometric Recalibration with the Stellar Color Regression Method and an Improved Gaia XP Synthetic Photometry Method. *Astrophys. J. Suppl. Ser.* **2023**, *269*, 58. [\[CrossRef\]](#)
156. Huang, Y.; Beers, T.C.; Xiao, K.; Yuan, H.; Lee, Y.S.; Gu, H.; Hong, J.; Liu, J.; Fan, Z.; Coelho, P.; et al. J-PLUS: Beyond Spectroscopy. III. Stellar Parameters and Elemental-abundance Ratios for Five Million Stars from DR3. *Astrophys. J.* **2024**, *974*, 192. [\[CrossRef\]](#)
157. Lu, X.; Yuan, H.; Xu, S.; Zhang, R.; Xiao, K.; Huang, Y.; Beers, T.C.; Hong, J. Stellar Loci. VII. Photometric Metallicities of 5 Million FGK Stars Based on GALEX GR6+7 AIS and Gaia EDR3. *Astrophys. J. Suppl. Ser.* **2024**, *271*, 26. [\[CrossRef\]](#)
158. Xiao, K.; Huang, Y.; Yuan, H.; Beers, T.C.; Huang, B.; Xu, S.; Yang, L.; Almeida-Fernandes, F.; Perottoni, H.D.; Limberg, G.; et al. S-PLUS: Photometric Recalibration with the Stellar Color Regression Method and an Improved Gaia XP Synthetic Photometry Method. *Astrophys. J. Suppl. Ser.* **2024**, *271*, 41. [\[CrossRef\]](#)

159. Gu, H.; Fan, Z.; Zhao, G.; Yang, H.; Beers, T.C.; Wang, W.; Zheng, J.; Zhao, J.; Li, C.; Chen, Y.; et al. The Stellar Abundances and Galactic Evolution Survey (SAGES). II. Machine Learning-based Stellar Parameters for 21 Million Stars from the First Data Release. *Astrophys. J. Suppl. Ser.* **2025**, *277*, 19. [\[CrossRef\]](#)
160. Huang, Y.; Beers, T.C. Stellar Parameters for over 50 Million Stars from SMSS DR4 and Gaia DR3. *Res. Notes Am. Astron. Soc.* **2025**, *9*, 74. [\[CrossRef\]](#)
161. Zhang, B.; Huang, Y.; Beers, T.C.; Xiao, K.; Liu, J.; Jia, L.; Han, H.; Li, Z.; Zheng, C.; Sun, Y.; et al. Photometric Stellar Parameters for 195,478 Kepler Input Catalog Stars. *Astrophys. J. Suppl. Ser.* **2025**, *277*, 6. [\[CrossRef\]](#)
162. Zheng, J.; Zhao, G.; Wang, W.; Fan, Z.; Tan, K.F.; Li, C.; Zuo, F. The SAGE photometric survey: Technical description. *Res. Astron. Astrophys.* **2018**, *18*, 147. [\[CrossRef\]](#)
163. Fan, Z.; Zhao, G.; Wang, W.; Zheng, J.; Zhao, J.; Li, C.; Chen, Y.; Yuan, H.; Li, H.; Tan, K.; et al. The Stellar Abundances and Galactic Evolution Survey (SAGES). I. General Description and the First Data Release (DR1). *Astrophys. J. Suppl. Ser.* **2023**, *268*, 9. [\[CrossRef\]](#)
164. Keller, S.C.; Schmidt, B.P.; Bessell, M.S.; Conroy, P.G.; Francis, P.; Granlund, A.; Kowald, E.; Oates, A.P.; Martin-Jones, T.; Preston, T.; et al. The SkyMapper Telescope and The Southern Sky Survey. *Publ. Astron. Soc. Aust.* **2007**, *24*, 1–12. [\[CrossRef\]](#)
165. Onken, C.A.; Wolf, C.; Bessell, M.S.; Chang, S.W.; Luvaul, L.C.; Tonry, J.L.; White, M.C.; Da Costa, G.S. SkyMapper Southern Survey: Data release 4. *Publ. Astron. Soc. Aust.* **2024**, *41*, e061. [\[CrossRef\]](#)
166. Mendes de Oliveira, C.; Ribeiro, T.; Schoenell, W.; Kanaan, A.; Overzier, R.A.; Molino, A.; Sampedro, L.; Coelho, P.; Barbosa, C.E.; Cortesi, A.; et al. The Southern Photometric Local Universe Survey (S-PLUS): Improved SEDs, morphologies, and redshifts with 12 optical filters. *Mon. Not. R. Astron. Soc.* **2019**, *489*, 241–267. [\[CrossRef\]](#)
167. Cenarro, A.J.; Moles, M.; Cristóbal-Hornillos, D.; Marín-Franch, A.; Ederoclite, A.; Varela, J.; López-Sanjuan, C.; Hernández-Monteagudo, C.; Angulo, R.E.; Vázquez Ramió, H.; et al. J-PLUS: The Javalambre Photometric Local Universe Survey. *Astron. Astrophys.* **2019**, *622*, A176. [\[CrossRef\]](#)
168. Perottoni, H.D.; Placco, V.M.; Almeida-Fernandes, F.; Herpich, F.R.; Rossi, S.; Beers, T.C.; Smiljanic, R.; Amarante, J.A.S.; Limberg, G.; Werle, A.; et al. The S-PLUS Ultra-Short Survey: First data release. *Astron. Astrophys.* **2024**, *691*, A138. [\[CrossRef\]](#)
169. Bonoli, S.; Marín-Franch, A.; Varela, J.; Vázquez Ramió, H.; Abramo, L.R.; Cenarro, A.J.; Dupke, R.A.; Vílchez, J.M.; Cristóbal-Hornillos, D.; González Delgado, R.M.; et al. The miniJPAS survey: A preview of the Universe in 56 colors. *Astron. Astrophys.* **2021**, *653*, A31. [\[CrossRef\]](#)
170. Barbosa, F.O.; Chiti, A.; Limberg, G.; Pace, A.; Cerny, W.; Rossi, S.; Carlin, J.L.; Stringfellow, G.; Placco, V.; Atzerberg, K.; et al. The DECam MAGIC Survey: A Wide-field Photometric Metallicity Study of the Sculptor Dwarf Spheroidal Galaxy. *arXiv* **2025**, arXiv:2504.03593. [\[CrossRef\]](#)
171. LSST Science Collaboration; Abell, P.A.; Allison, J.; Anderson, S.F.; Andrew, J.R.; Angel, J.R.P.; Armus, L.; Arnett, D.; Asztalos, S.J.; Axelrod, T.S.; et al. LSST Science Book, Version 2.0. *arXiv* **2009**, arXiv:0912.0201. [\[CrossRef\]](#)
172. Ivezić, Ž.; Kahn, S.M.; Tyson, J.A.; Abel, B.; Acosta, E.; Allsman, R.; Alonso, D.; AlSayyad, Y.; Anderson, S.F.; Andrew, J.; et al. LSST: From Science Drivers to Reference Design and Anticipated Data Products. *Astrophys. J.* **2019**, *873*, 111. [\[CrossRef\]](#)
173. Mumpower, M.R.; Surman, R.; McLaughlin, G.C.; Aprahamian, A. The impact of individual nuclear properties on r-process nucleosynthesis. *Prog. Part. Nucl. Phys.* **2016**, *86*, 86–126. [\[CrossRef\]](#)
174. Horowitz, C.J. Neutron rich matter in the laboratory and in the heavens after GW170817. *Ann. Phys.* **2019**, *411*, 167992. [\[CrossRef\]](#)

Disclaimer/Publisher’s Note: The statements, opinions and data contained in all publications are solely those of the individual author(s) and contributor(s) and not of MDPI and/or the editor(s). MDPI and/or the editor(s) disclaim responsibility for any injury to people or property resulting from any ideas, methods, instructions or products referred to in the content.